RMP Colloquia

Coherent population transfer among quantum states of atoms and molecules

K. Bergmann, H. Theuer, and B. W. Shore*

Fachbereich Physik der Universität Kaiserslautern, 67653 Kaiserslautern, Germany

The authors discuss the technique of stimulated Raman adiabatic passage (STIRAP), a method of using partially overlapping pulses (from pump and Stokes lasers) to produce complete population transfer between two quantum states of an atom or molecule. The procedure relies on the initial creation of a coherence (a population-trapping state) with subsequent adiabatic evolution. The authors present the basic theory, with some extensions, and then describe examples of experimental utilization. They note some applications of the technique not only to preparation of selected states for reaction studies, but also to quantum optics and atom optics. [S0034-6861(98)00803-4]

CONTENTS

*Permanent address: Lawrence Livermore National Laboratory, Livermore CA 94550.

I. INTRODUCTION

The notion of transitions between individual discrete quantum states is central to the study of time-evolving quantum systems. For example, chemical reactions in the bulk are the result of a thermal average over many distinct state-to-state transitions. Although the thermal averaging blurs the characteristic features of the dynamics, these individual processes need to be resolved if one is to understand the reaction rate. Therefore there has long been interest in finding techniques with which to control the transfer of population between specified quantum states.

This article describes a recently developed technique that permits precise control of population transfer (for a review, see Bergmann and Shore, 1995). The scheme, which relies upon at least two coherent pulses of light, allows complete transfer of population between two suitable quantum states. As we shall point out, the use of two lasers coupling three states, rather than a single laser coupling two states, offers many advantages: the excitation efficiency can be made relatively insensitive to many of the experimental details of the pulses. In addition, with the three-state system, one can produce excitation between states of the same parity, for which single-photon transitions are forbidden for electric-dipole radiation, or between magnetic sublevels.

In simplest form, the scheme involves a three-state, two-photon Raman process, in which an interaction with a pump pulse P links the initial state $|1\rangle$ with an intermediate state $|2\rangle$, which in turn interacts via a Stokes pulse S with a final, target, state $|3\rangle$. Figure 1 illustrates the connections. Typically state $|1\rangle$ might be a rotational level in the vibrational ground state of a molecule, and state $|3\rangle$ might be a highly excited vibrational state. Al-

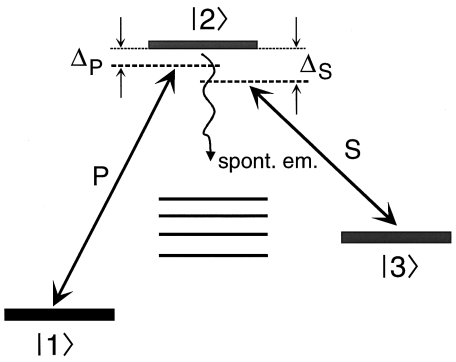

FIG. 1. Three-level excitation scheme. The initially populated state $|1\rangle$ and the final state $|3\rangle$ are coupled by the Stokes laser S and the pump laser P via an intermediate state $|2\rangle$. This latter state may decay by spontaneous emission to other levels. The detuning of the pump and Stokes laser frequencies from the transition frequency to the intermediate state are Δ_P and Δ_S, respectively.

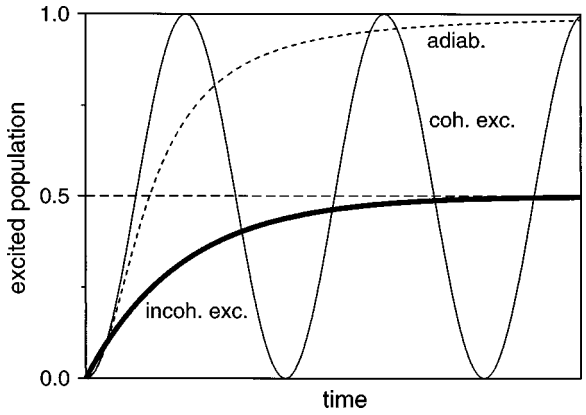

FIG. 2. Evolution of the population of the upper level in a two-level system, driven by a coherent radiation field (thin line), by an incoherent radiation field (heavy line), and by an adiabatic passage process (dashed line).

ternatively, these could be metastable atomic states whose lifetimes are long compared with the length of a laser pulse.

The initial and final states must be long lived, whereas the intermediate state will undergo spontaneous emission not only to states $|1\rangle$ and $|3\rangle$, but also to other states. The objective is to transfer all of the population from state $|1\rangle$ into state $|3\rangle$, losing none by spontaneous emission from state $|2\rangle$.

At first glance, the possibility of radiative decay from the intermediate level to states other than the desired final state seems to be detrimental to the implementation of an efficient transfer to a single quantum state. However, as we shall see, the STIRAP process to be discussed has the remarkable property of placing almost no population into the intermediate state $|2\rangle$, and thus it is insensitive to any possible decay from that state.

Coupling is strongest when the individual laser frequencies are tuned to their respective resonance frequencies, but such one-photon frequencies are not needed; it is only necessary that the combination of pump and Stokes frequencies be resonant with the two-photon Raman transition.

The remarkable properties of this scheme have already had applications in such diverse areas as chemical-reaction dynamics (Dittmann *et al.*, 1992), laser-induced cooling (Kulin *et al.*, 1997a), atom optics (Weitz, Young, and Chu, 1994), and cavity quantum electrodynamics (Parkins *et al.*, 1993; Walser, Cirac, and Zoller, 1996).

In the following, we shall first discuss some basic aspects of the interaction of radiation with a two-state system, to stress the importance of coherence. We shall then move on to discuss three-state and multistate problems. We provide, in the Appendices, further details of the theoretical extension of the original STIRAP process and of experimental studies in a variety of atomic and molecular systems.

II. SOME PROPERTIES OF TWO-STATE SYSTEMS

Given the task of transferring population from a thermally occupied quantum state to an empty one, we may choose one of many processes. Collisional interactions of various kinds (with neutral or charged particles) can serve the purpose. However, these processes are either inefficient or lack selectivity, i.e., more than one final state is populated. The most obvious choice for state-selective excitation is the absorption of one or several photons which together match the energy difference between the quantum states. The resulting population depends critically upon the coherence characteristics of the light. Differences in coherence cause differences in the excitation dynamics and, in turn, require different equations to describe time evolution (Shore 1990, Chap. 2). To illustrate the range of differences, Fig. 2 presents examples of excitation histories of population for three kinds of radiative excitation.

(a) *Incoherent excitation.* To quantify excitation involving incoherent light one uses differential equations for excitation probabilities (rate equations; Shore, 1990, Sec. 2.2). Assuming that the atoms are in the lower of two states (the ground state) at time $t=0$, and that stimulated emission dominates spontaneous emission, one finds the excitation probability (of being in the upper state) at time t to be

$$P_{ex}(t)=\tfrac{1}{2}\{1-\exp[-\alpha F(t)]\}, \tag{1}$$

where α is the absorption coefficient. The pulse fluence $F(t)$ (energy per unit area) is the integral of the time-varying intensity $I(t)$ (power per unit area) over the pulse duration,

$$F(t)=\int_{-\infty}^{t} I(t')dt'. \tag{2}$$

This expression for population transfer approaches, monotonically in time, the saturation value of 0.5 for long times. Such behavior is shown as the heavy line of Fig. 2. As can be seen, the population transfer to the excited state levels off (saturates) at 50%.

(b) *Coherent excitation.* By contrast, quantitative discussions of coherent excitation start from a time-dependent Schrödinger equation (for probability

amplitudes)[1] with an appropriate interaction Hamiltonian (Shore, 1990, Sec. 2.7). The basic equation is

$$\frac{d}{dt}\mathbf{C}(t) = -\frac{i}{\hbar}\mathsf{H}(t)\mathbf{C}(t), \tag{3}$$

where $\mathbf{C}(t)$ is a vector of time-dependent probability amplitudes $C_1(t), \ldots, C_n(t), \ldots$, whose absolute squares provide the probability $P_n(t) = |C_n(t)|^2$ of finding the system at time t in state $|n\rangle$. The time evolution of these functions is dictated by the Hamiltonian matrix $\mathsf{H}(t)$. Typically we assume that all population resides initially in state 1, and we require the excitation probability $P_{ex}(t) \equiv P_N(t)$ of finding the system much later in a specified target state N.

For radiative transitions the excitation is induced by an electric field acting upon a transition dipole moment. One idealizes the radiation as a nearly monochromatic field, of frequency ω, having magnitude $\mathcal{E}(t)\cos(\omega t)$, with $\mathcal{E}(t)$ either constant (for cw radiation) or a slowly varying envelope (for pulsed excitation). With incoherent radiation the key quantifier of radiation is the instantaneous intensity $I(t) = |\mathcal{E}(t)|^2 c\epsilon_0/2$ (in SI units). For coherent radiation the key parameter is the Rabi frequency (basically the interaction energy converted to frequency),

$$\Omega(t) = \frac{\mu\mathcal{E}(t)}{\hbar}, \tag{4}$$

where $\mathcal{E}(t)$ is the envelope of the electric-field amplitude at the location of the atom or molecule and μ is the component of the transition dipole moment along the electric field. For resonant radiation acting on a two-state system the excitation probability (for $N=2$) is

$$P_{ex}(t) = [\sin \tfrac{1}{2}A(t)]^2 = \tfrac{1}{2}[1 + \cos A(t)], \tag{5}$$

where $A(t)$ is the pulse area up to time t,

$$A(t) = \int_{-\infty}^{t} \Omega(t')dt'. \tag{6}$$

This population undergoes sinusoidal variation, alternately reaching 100% and 0%. The frequency of these oscillations is the Rabi frequency. In particular, the excitation probability reaches a maximum value whenever $A(t) = (2n+1)\pi$ (a multiple π pulse). The thin line of Fig. 2 shows the behavior of a two-state system when exposed to coherent radiation (again tuned to the resonance frequency). When averaged over many Rabi cycles the population is again shared equally by the two states.

Although we do not explicitly indicate this, the transition dipole moment μ depends on the quantum numbers of the states involved. In particular, the interaction strength depends upon the component of the dipole moment along the electric-field vector, as expressed by a dependence upon the magnetic quantum number m. For degenerate magnetic sublevels, the observed excitation is an average over possible atomic orientations, each with a different Rabi frequency (and hence a different pulse area). Because the electric-field strength varies over the cross section of the laser beam, different atom trajectories experience further variation of the excitation probability. As a result of these variations of pulse area in typical experimental conditions, the π-pulse technique, which requires a precise value of the pulse area, will be the method of choice only for some specific problems.

(c) *Adiabatic transfer.* In order to achieve more efficient and uniform excitation probabilities than those just described, one can utilize coherent pulses whose frequency sweeps slowly across the resonance (adiabatic passage), or one can employ other variants of adiabatic change, to be described below. With such schemes one can obtain efficient and selective population transfer of the sort shown as a dashed line in Fig. 2. Applications of these techniques to three-state (or multistate) systems pose a more challenging task.

III. PROCESSES IN A THREE-STATE SYSTEM

A. Stimulated emission pumping

The importance of illuminating with coherent radiation (i.e., the advantage of laser light compared with narrow-bandwidth thermal radiation) becomes even more evident as one considers excitation involving more than two energy states. A popular successful method for the transfer of population in a three-level system is the technique of stimulated emission pumping (SEP) (Hamilton, Kinsey, and Field, 1986). Because coherence properties of the radiation are not relevant in this case, the excitation can be treated in the framework of rate equations (Bergmann and Shore, 1995).[2] With SEP the pump laser (see Fig. 1) acts first, followed, after some time delay, by the dump (or Stokes) laser. If the laser intensities are sufficiently high to saturate the respective transitions, then 50% of the population of level $|1\rangle$ is found in level $|2\rangle$ at the end of the pump interaction (as shown for the two-state system in Fig. 2). If the Stokes laser is also strong enough, the population of level $|2\rangle$ is subsequently dumped into level $|3\rangle$. Therefore typically half of the population remains in the ground level, a quarter of the population is transferred to level $|3\rangle$, while another quarter will reach other levels by spontaneous radiative decay. Because SEP is relatively easy to implement, it has enjoyed widespread application to problems in collision dynamics and spectroscopy (Dai

[1]It is important to recognize that, whereas incoherent rate equations apply to degenerate energy levels, possibly comprising several states, the Schrödinger equation applies to nondegenerate quantum states.

[2]In particular, the radiative transitions may occur between degenerate levels, rather than simply between nondegenerate quantum states.

and Field, 1994). The lack of high selectivity is the main limitation of the SEP technique in some applications.

B. The eigenstates of coherently coupled systems

An interesting and far-reaching alternative to the SEP scheme, one which exploits the coherence of the radiation fields to achieve complete population transfer, will now be discussed. Rather than exposing the atom or molecule to the pump laser first and then to the Stokes laser, one reverses the ordering of the pulse sequence: the system first interacts with the Stokes laser and then with the pump laser (and there must be an appropriate overlap between the two). What seems counterintuitive at first glance becomes the natural choice when the consequences of coherence are considered. Initially, the Stokes laser couples the two empty states, and thus it does not change the population of state $|1\rangle$. However, this does not mean that the Stokes laser has no effect. In fact, this laser creates a coherent superposition of the two initially unpopulated states $|2\rangle$ and $|3\rangle$. When this coherent superposition state is subsequently coupled to the populated state $|1\rangle$ by the pump laser, a "trapped state" is formed—a state from which the pump laser cannot transfer population to the radiatively decaying intermediate state. Rather, the population is directly channeled into state $|3\rangle$, as the discussion and the equation below reveal. [The properties of trapped states have recently been reviewed by Arimondo (1996)].

For the simplest implementation of STIRAP, the Hamiltonian, which describes the coupling of the three states (nondegenerate levels) by two coherent radiation fields within the rotating wave approximation (RWA; Shore, 1990, Sec. 13.7), reads

$$\mathsf{H}(t)=\frac{\hbar}{2}\begin{bmatrix} 0 & \Omega_P(t) & 0 \\ \Omega_P(t) & 2\Delta_P & \Omega_S(t) \\ 0 & \Omega_S(t) & 2(\Delta_P-\Delta_S) \end{bmatrix}. \tag{7}$$

The coupling strength between the states is determined by the pulsed Rabi frequencies $\Omega_S(t)$ and $\Omega_P(t)$, while the detuning from the intermediate state or from the two-photon resonance appears as the elements on the diagonal: $\hbar\Delta_P=(E_2-E_1)-\hbar\omega_P$ is the detuning (energy) of the pump laser from resonance with the $|2\rangle$-$|1\rangle$ transition and $\hbar\Delta_S=(E_2-E_3)-\hbar\omega_S$ is the detuning of the Stokes laser from the $|2\rangle$-$|3\rangle$ transition. Although the presence of these single-photon detunings does not prevent population transfer, it is essential that the two-photon resonance condition $\Delta_P=\Delta_S$ apply (for a discussion of the two-photon linewidth in this situation, see Romanenko and Yatsenko, 1997).

The actions of the coherent radiation fields are included in the Hamiltonian of Eq. (7), but spontaneous radiative decay is not. Because one is interested in producing transitions between states $|1\rangle$ and $|3\rangle$ that have much longer lifetimes than the pulse duration, only decay of $|2\rangle$ needs to be considered. When using the Schrödinger equation to describe time evolution, we can account for some decay processes by making the excited-state energy a complex number: the imaginary part is the decay rate into states other than the states $|1\rangle$ *and* $|3\rangle$. A more complete description, allowing for decays into $|1\rangle$ and $|3\rangle$, requires a more elaborate and rigorous treatment based on the density-matrix formalism (see Shore, 1990, Sec. 6.4). Radiative decay is important because it serves as a leak responsible for loss of population from the three-state system. Population lost by spontaneous emission reaches states that one wishes would remain unpopulated.

The rotating wave approximation neglects terms in the Schrödinger equation that oscillate in time with sums and differences of the two carrier frequencies. This approximation is well justified for the examples discussed in this article. The relevant frequency components are not tuned far off resonance with the respective one-photon transition and (in a three-state system) each of the two lasers interacts with only one pair of states. The latter requirement demands that the separation in energy of the initial and final state be large compared to either the laser bandwidth or the Rabi frequency (whichever is larger) unless the interaction of the pump and Stokes laser is restricted to one pair of states by optical selection rules (see Appendices A and C2). The former requirement is well satisfied for continuous single-frequency lasers and for pulsed lasers, provided the pulse length is not too short. The large spectral bandwidth of laser pulses in the femtosecond regime may invalidate the RWA.

In the following, we discuss the dynamics of coherent excitation in the basis of time-dependent eigenstates of the RWA Hamiltonian of Eq. (7). It is straightforward to verify that the following linear combinations of the bare states $|1\rangle$, $|2\rangle$, and $|3\rangle$ are eigenstates of the instantaneous RWA Hamiltonian of Eq. (7):

$$\begin{aligned} |a^+\rangle &= \sin\Theta\,\sin\Phi|1\rangle+\cos\Phi|2\rangle+\cos\Theta\,\sin\Phi|3\rangle, \\ |a^0\rangle &= \cos\Theta|1\rangle-\sin\Theta|3\rangle, \\ |a^-\rangle &= \sin\Theta\,\cos\Phi|1\rangle-\sin\Phi|2\rangle+\cos\Theta\,\cos\Phi|3\rangle, \end{aligned} \tag{8}$$

where the (time-varying) mixing angle Θ is defined by the relationship

$$\tan\Theta=\frac{\Omega_P(t)}{\Omega_S(t)}. \tag{9}$$

The angle Φ is a known function of the Rabi frequencies and detunings and is of no relevance to the subsequent discussion (Fewell, Shore, and Bergmann, 1997). The eigenstates given by Eq. (8) are valid for the case of two-photon resonance (for a discussion of the more general case, see Fewell *et al.*, 1997). When combined with the related photon numbers in the two radiation fields, these states are called the "dressed states" of the matter-field system. Although we do not keep track of the photon numbers, we use this name here as well. The (time-dependent) dressed-state eigenvalues are

$$\begin{aligned} \omega^+ &= \Delta_P+\sqrt{\Delta_P^2+\Omega_P^2+\Omega_S^2}, \quad \omega^0=0, \\ \omega^- &= \Delta_P-\sqrt{\Delta_P^2+\Omega_P^2+\Omega_S^2}. \end{aligned} \tag{10}$$

C. The transfer process

The objective is to control the state vector $|\psi\rangle$, thereby controlling the distribution of population among the three states. At very early times, $|\psi\rangle$ will be identical to $|1\rangle$. At very late times, we require that $|\psi\rangle$ be parallel to $|3\rangle$. We wish to avoid even transient placement of population into $|2\rangle$, which will radiatively decay to other states that are not connected by the coherent radiation fields.

Equations (8) and (10) are the basis of the subsequent discussion of the transfer process. The eigenstates $|a^+\rangle$ and $|a^-\rangle$ are represented by a linear combination of all three bare states. They include, in particular, a component of the bare state $|2\rangle$, which is the leaky state. We therefore wish to avoid population in either of these two dressed states, whether produced directly or by nonadiabatic coupling during the process.

The state $|a^0\rangle$ is, at all times, free of any contribution from the leaky state $|2\rangle$, and thus it will be the appropriate vehicle for transferring population from state $|1\rangle$ to state $|3\rangle$ without populating state $|2\rangle$. Equations (8) and (9) reveal how this can be done. The mixing angle Θ can be experimentally controlled through the ratio of the Rabi frequencies, Eq. (9). Specifically, if the Stokes laser precedes the pump laser, as shown in Fig. 3, we identify three distinctly different intervals I, II, and III. In region I, only the Stokes laser is present; the Rabi frequency due to the pump laser is zero, i.e., the mixing angle is zero. Therefore, as the atoms or molecules are exposed to the Stokes laser (only), the state $|a^0\rangle$ is identical to state $|1\rangle$ as well as to the state vector $|\psi\rangle$. Thus, in region I, three vectors are aligned: the vector representing the bare state $|1\rangle$, the vector $|a^0\rangle$ of the strongly coupled system, and the state vector $|\psi\rangle$ (see Fig. 4). In the interval II the Stokes laser Rabi frequency is smoothly reduced while the pump laser Rabi frequency increases to its maximum value, changing the mixing angle smoothly from 0° to 90°. As shown in Fig. 4, the vector $|a^0\rangle$ is rotated into a position parallel to the bare state $|3\rangle$ in a plane perpendicular to the bare state $|2\rangle$. Therefore, during this motion, the vector never acquires a component of the leaky state $|2\rangle$. The crucial question, discussed in the next section, is whether or not the coupling of the states by the radiation fields is strong enough that the flow of population (or the state vector $|\psi\rangle$) follows the motion of the vector $|a^0\rangle$ adiabatically.

We can also understand the evolution of the system by looking at the dressed-state eigenvalues [see Fig. 3(c)]. Consider the case of resonant tuning of both lasers to their respective transition frequency. At very early times, when both Rabi frequencies are zero, all three eigenvalues are degenerate. As we shall see, this condition is not harmful to the transfer process. During interval I, the Stokes laser couples states $|2\rangle$ and $|3\rangle$ while state $|1\rangle$ is not involved in the interaction. At this time, therefore, the splitting of the eigenvalues is due to the coupling of states $|2\rangle$ and $|3\rangle$ alone. The eigenvalue that remains unchanged is associated with $|a^0\rangle$ (which is identical to state $|1\rangle$ at this early time). The vector $|a^0\rangle$

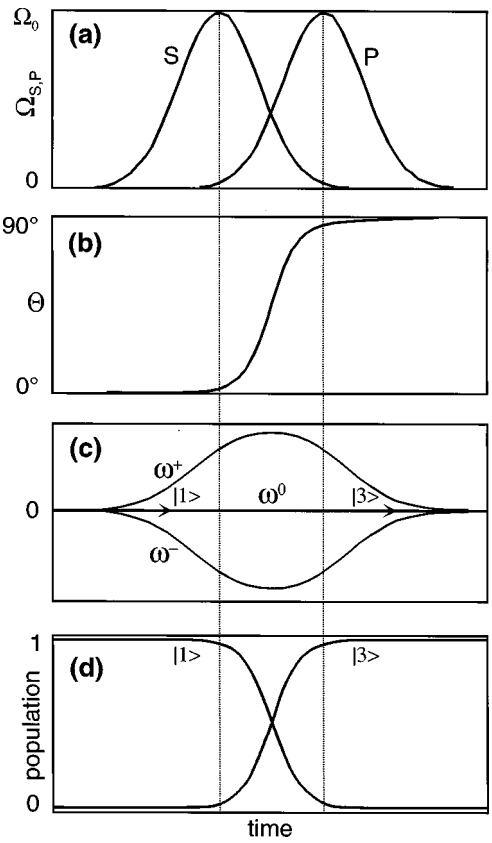

FIG. 3. Time evolution of (a) the Rabi frequencies of the pump and Stokes laser (see Fig. 1); (b) the mixing angle [see Eq. (9)]; (c) the dressed-state eigenvalues [see Eq. (10)]; and (d) the population of the initial level (starting at unity) and the final level (reaching unity).

still remains in its original position (Fig. 4), but the degeneracy with the eigenvalues of states $|a^+\rangle$ and $|a^-\rangle$ is lifted. During interval II, the splitting of the eigenvalues ω^+,ω^-, and ω^0 is largest, i.e. the coupling is strongest and both radiation fields contribute to it, as the vector moves from its position parallel to state $|1\rangle$ into the position parallel to state $|3\rangle$. This motion results in complete population transfer if the state vector $|\psi\rangle$ evolves adiabatically. If the coupling is insufficient (i.e., if the Rabi frequencies are too small), the motion of the state vector $|\psi\rangle$ will lag behind the motion of the dressed states; it will precess around $|a^o\rangle$. It is qualitatively obvious that the state vector then acquires a component along $|a^+\rangle$ or $|a^-\rangle$ (by nonadiabatic coupling). This implies that some population reaches the leaky state $|2\rangle$ and that the transfer process will be incomplete. The relevance of nonadiabatic coupling among the dressed states due to the explicit time dependence of the Hamiltonian needs to be carefully evaluated. This will be done in Sec. V.

Based on the discussion above, it should now be obvious that the method of coherent population transfer combines features of the process of stimulated Raman scattering and adiabatic passage, which justifies the acronym STIRAP.

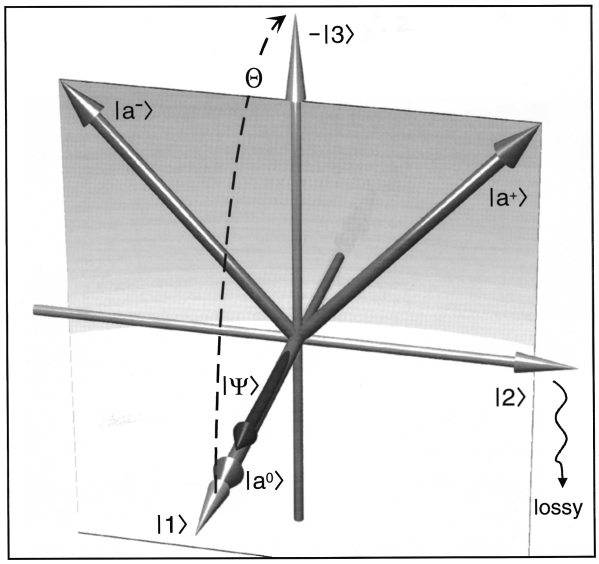

FIG. 4. Graphic representation of the Hilbert space for the three-level system in the basis of the bare states ($|1\rangle$, $|2\rangle$, and $|3\rangle$) and in the basis of the dressed states $|a^0\rangle$, $|a^+\rangle$, and $|a^-\rangle$. When the Stokes laser is much stronger than the pump laser (phase I, see Fig. 3), the state vectors $|1\rangle$ and $|a^0\rangle$ are aligned parallel to each other. Since the population is initially in state $|1\rangle$, the state vector is also aligned parallel to $|1\rangle$. At later times, the components of the state vector along the three dressed or bare states give the population in these states.

IV. EXPERIMENTAL DEMONSTRATION FOR A THREE-LEVEL SYSTEM

Before we expand further on the theoretical analysis (Sec. V), we first discuss experimental data that exemplify basic features of the coherent population transfer process by delayed pulses. When continuous lasers are used in combination with atomic or molecular beams, it is straightforward to expose the molecules to a delayed sequence of interactions simply by spatially displacing the axes of the laser beams (see Fig. 5). When pulsed lasers are used, the axes of the laser beams need to coincide but the pulses must be delayed in time.

A. Experimental arrangement

The metastable states of neon (Ne*) provide a convenient system for the study of basic properties of coherent population transfer (see Fig. 6). The electronic configuration $2p^5 3s$ leads to two metastable levels, $^3P_0$ and $^3P_2$, which are connected by one-photon dipole transitions to other levels in the $2p^5 3p$ configuration, with resonance wavelength near 600 nm, as shown in the figure. The $2p^5 3p(^3P_1)$ level was chosen to provide the intermediate state for the transfer process. This state, as well as other states of the $2p^5 3p$ configuration, radiatively couples to the $^1P_1$ or $^3P_1$ levels of the $2p^5 3s$ configuration. Subsequent decay to the ground state of the atom leads to the emission of a vacuum-ultraviolet (vuv) photon (wavelength 74 nm), which can be detected easily by a channeltron detector with little, if any, background signal. In fact, this vuv radiation is used not

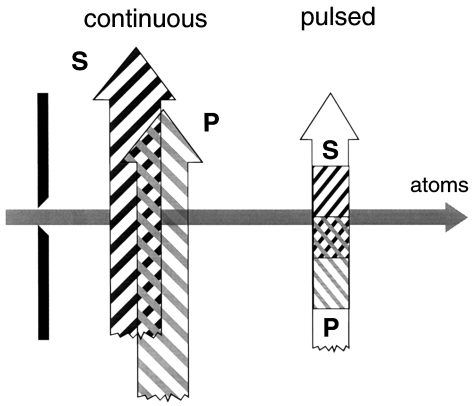

FIG. 5. Schematics of the STIRAP setup for population transfer for particles in a molecular beam. When continuous laser radiation is used, the STIRAP sequences (Stokes before pump) is implemented by spatially shifting the axes of the S and P lasers relative to each other. When pulsed lasers are used, the STIRAP sequence is implemented by appropriate time delay of the pulses.

only to detect emission from the intermediate level $^3P_1$ but also to monitor the population of the metastable states by laser-induced fluorescence.

In our experiments, a beam of Ne* atoms emerges from a discharge source (see Fig. 7) into a vacuum. A preparation laser depletes the population of one of the metastable levels by optical pumping. Excitation of the $^3P_2$ level (for instance, to the $^3D_2$ level) results in emission to the short-lived levels of the $2p^5 3s$ configuration followed by decay to the ground state.

After passing through a collimating slit, the atoms (those in the $^3P_0$ state together with those in the electronic ground state, which are of no further relevance in this context) travel through the STIRAP zone, determined by the Stokes and the pump laser, with their axes suitably displaced. In the region where these laser beams spatially overlap, the population of the $^3P_0$ state is

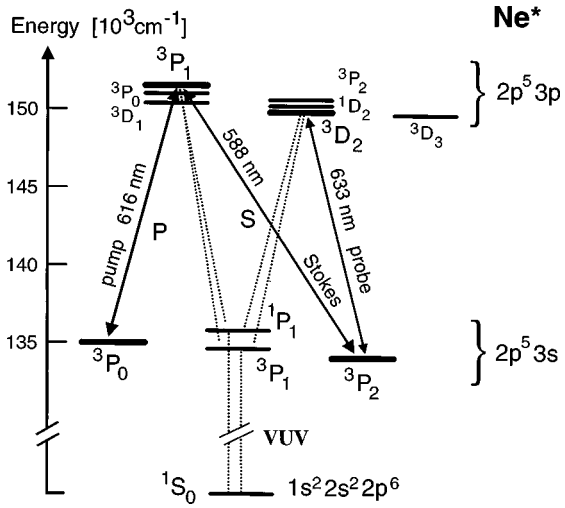

FIG. 6. Levels and transition wavelength for the Ne atom, relevant for some of the work presented here.

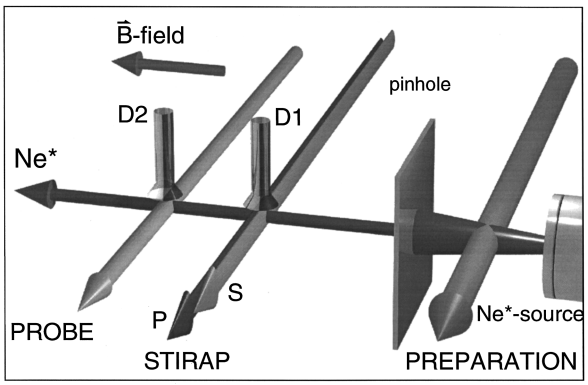

FIG. 7. Schematics of the experimental arrangements for the Ne* experiments. The beam of metastable atoms emerges from a discharge source. If needed, the population of one of the metastable levels is eliminated by optical pumping (preparation laser). After collimation, the atomic beam reaches the ultrahigh vacuum region, and crosses the STIRAP transfer zone as well as the detection region. The fluorescence from the intermediate level in the transfer zone and the population in the final level, detected by the probe-laser-induced fluorescence, are monitored through the cascade vuv fluorescence (see Fig. 6). Channeltrons (D1 and D2) are positioned atop the crossings of the laser beams and the atomic beam to detect the vuv photons.

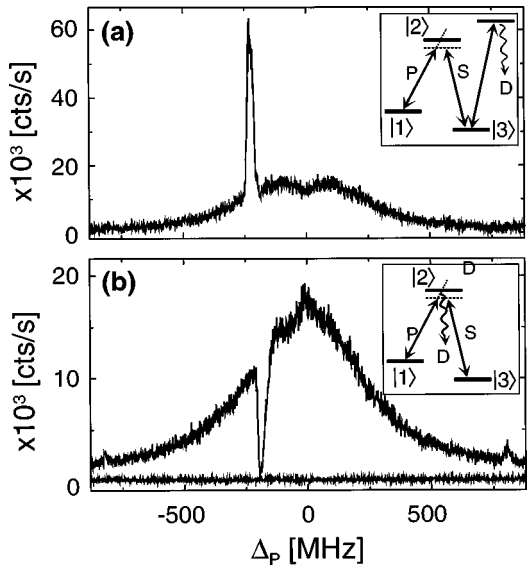

FIG. 8. Population transfer (upper panel), as well as related dark resonance (lower panel) as detected by the channeltron above the crossing of the molecular beam with the probe laser as well as the pump and Stokes laser, respectively. For further details, see text.

transferred to the other metastable level ($^3P_2$), with or without magnetic sublevel selectivity (see Appendix A). If the efficiency of the transfer process is less than unity, some transient population will reside in the intermediate level and fluorescence (emission of a vuv photon with an energy of 16.7 eV) will be observed at the detector D1. Downstream from the transfer zone, a probe laser excites atoms in the $^3P_2$ level. Again, it is the vuv radiation that is monitored by a channeltron detector (D2). The total flux of metastable atoms can also be detected further downstream by a third channeltron (D3) positioned on the axis of the atomic beam.

B. Population transfer and the dark resonance

Fluorescence measurements like that shown in Fig. 8 provide evidence for population transfer. Figure 8(a) shows laser-induced fluorescence as a function of pump laser frequency. This signal, monitored by detector D2, is proportional to the population of the $^3P_2$ level (state $|3\rangle$). Figure 8(b) shows the fluorescence from the intermediate level as the pump laser frequency is tuned, while the Stokes laser frequency, tuned slightly off resonance, remains unchanged.

The signal presented in Fig. 8(a) shows a broad feature, widened by strong saturation to exceed the natural linewidth (or the residual Doppler width) by an order of magnitude. As soon as the pump laser transfers some population into the intermediate state $|2\rangle$, a known fraction of it will reach state $|3\rangle$ by radiative decay. At a specific detuning of the pump laser frequency, the two-photon resonance condition is met and coherent population transfer occurs. When this happens, very little (if any) transient population will reside in level two and the fluorescence from the intermediate level (monitored by detector D1) disappears, as shown in Fig. 8(b). Thus efficient population transfer is accompanied by a pronounced dark resonance. In fact, residual fluorescence at the center of the dark resonance has been observed as low as 0.5% as compared to the fluorescence with the Stokes laser off (Theuer and Bergmann, 1998), despite the fact that the interaction time with the pump laser exceeds the radiative lifetime by more than a factor of 20.

C. The STIRAP signature

To prove that the population transfer occurs through the STIRAP mechanism, one must measure the transfer efficiency T as the overlap Δ between the laser beams is varied while all other parameters, such as laser frequencies and intensities, remain unchanged. Figure 9 shows an example of such variation in T. When the axis of the Stokes laser is shifted far upstream by more than the beam diameter, so that there is no overlap with the pump laser beam profile, the Stokes laser does not participate in the transfer process, since at no time do photons from both lasers simultaneously interact with the atom. The pump laser excites atoms from state $|1\rangle$ to the intermediate state from which they radiatively decay. A known fraction of the transient population of the intermediate state reaches state $|3\rangle$ (the rest falls back to state $|1\rangle$ and is again excited or is lost via the cascade transition to the ground state of the atom). Therefore the transfer efficiency is known relative to the signal when only the pump laser acts on the population in state $|1\rangle$.

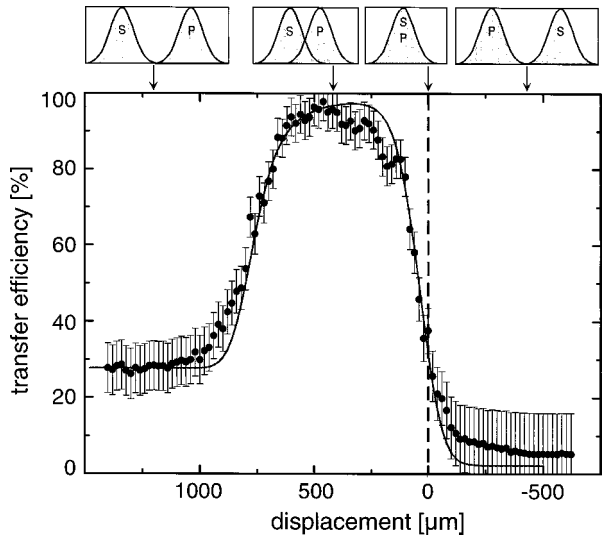

FIG. 9. Population transfer from the $^3P_0$ state to the $^3P_2$ state (see Fig. 6), induced by a continuous laser, as a function of the overlap between the Stokes and the pump lasers (shown on top).

As the axes of the Stokes and pump laser move closer together, the transfer efficiency increases dramatically and reaches (within the experimental uncertainty) the value of unity. When the axes of the two lasers coincide, the transfer efficiency is only of the order of 25%. Essentially no transfer is observed when the Stokes laser axis is moved farther downstream of the pump laser beam axis (see Sec. V). The experimental data are in very good agreement with the results from a numerical simulation study (solid line in Fig. 9). The latter results reveal that a transfer efficiency even closer to unity can be achieved when the power of the pump and Stokes laser is further increased. It is also obvious that the transfer efficiency reaches a plateau near the optimum delay. This is an indication of the robustness of the transfer process. In fact, the variation of the transfer efficiency with the delay of the interaction of the two lasers, shown in Fig. 9, is a characteristic signature of the STIRAP process.

V. ADIABATIC FOLLOWING

A. Condition for adiabatic following

As was pointed out in Sec. III, insufficient coupling by the coherent radiation fields may prevent the state vector $|\psi\rangle$ from adiabatically following the evolution of the trapped state $|a^0\rangle$ (see Fig. 4), and loss of population due to nonadiabatic transfer to the states $|a^+\rangle$ and $|a^-\rangle$ may occur. The condition for adiabatic following can be derived from general considerations in quantum mechanics which need to be invoked whenever the Hamiltonian is explicitly time dependent. The Hamiltonian matrix element for nonadiabatic coupling between state $|a^0\rangle$, which carries the population and evolves in time, and either one of the states $|a^+\rangle$ or $|a^-\rangle$ is given by $\langle a^\pm|\dot{a}^0\rangle$ (Messiah, 1961). Nonadiabatic coupling is small if this matrix element is small compared to the field-induced splitting $|\omega^\pm-\omega^0|$ of the energies of these states, i.e.,

$$|\langle a^+|\dot{a}^0\rangle| \ll |\omega^\pm-\omega^0|. \tag{11}$$

Using Eqs. (10) to express the coupling strengths in Eq. (11), we find $\langle a^+|\dot{a}^o\rangle=-\dot{\Theta}\sin\Phi$, and therefore the adiabaticity constraint, with $\sin\Phi=1$, reads

$$|\dot{\Theta}| \ll |\omega^\pm-\omega^0|. \tag{12}$$

Using Eq. (9) it is easy to show that Eq. (12) can be written in the form (Kuklinski *et al.*, 1989)

$$\left|\frac{\dot{\Omega}_P\Omega_S-\Omega_P\dot{\Omega}_S}{\Omega_P^2+\Omega_S^2}\right| \ll |\omega^\pm-\omega^0|. \tag{13}$$

We may consider Eq. (13) to be a "local" adiabaticity criterion, because, for a given shape of the laser pulses, both sides can be evaluated at any time t. Nonadiabatic coupling of the state $|a^0\rangle$ to the states $|a^+\rangle$ or $|a^-\rangle$ is small if the condition imposed by Eq. (13) is satisfied throughout the interaction.

When the laser pulses have a smooth shape, a convenient "global" adiabaticity criterion may be derived from Eq. (12) by taking a time average of the left-hand side, $\langle\dot{\Theta}_{av}\rangle=\pi/2\Delta\tau$, where $\Delta\tau$ is the period during which the pulses overlap. This should not exceed the value of the right-hand side, $|\omega^\pm-\omega^0|=\Omega_{eff}$, where $\Omega_{eff}=\sqrt{\Omega_P^2+\Omega_S^2}$ is the rms Rabi frequency. This procedure leads to the condition

$$\Omega_{eff}\Delta\tau > 10, \tag{14}$$

where the numerical value of 10 on the right-hand side was obtained from experience and numerical simulation studies.

B. Optimum pulse delay

It has been shown (Gaubatz *et al.*, 1990) that for a Gaussian-beam pulse shape the lowest losses from nonadiabatic coupling to the $|a^+\rangle$ or $|a^-\rangle$ states are achieved when the delay equals the laser pulse width. Here we discuss qualitatively the reasons behind that finding.

The objective of the delayed-pulse scheme is to maximize the projection of the vector representing the bare state $|1\rangle$ onto the state $|a^0\rangle$. For overlapping pulses we have $\dot{\Theta}=0$, i.e., Eq. (12) would be trivially fulfilled. However, state $|1\rangle$ has nonvanishing components along all three states, $|a^+\rangle$, $|a^-\rangle$, and $|a^0\rangle$, [see Eq. (8)]. Only the projection on $|a^0\rangle$ can be used for efficient population transfer, because population of the other states may be lost through radiative decay. Indeed, all of the population in $|a^+\rangle$ or $|a^-\rangle$ will be lost if the radiative lifetime is short compared to $\Delta\tau$. Furthermore, at the end of the interaction, only a fraction of the population in $|a^0\rangle$ will be found in state $|3\rangle$, i.e., $|\langle 3|a^0\rangle|$ is less than unity. Thus for zero delay the transfer efficiency from state $|1\rangle$ to state $|3\rangle$ is limited to about 25%, as confirmed by the result shown in Fig. 9.

For large delay $|\langle 1|a^0\rangle|$ approaches unity because $\Omega_S \gg \Omega_P$ at early times. However, if the delay is too large, the maximum rate of change of the mixing angle Θ occurs when Ω_{eff} has fallen below its maximum value, i.e., when the radiative coupling (or the Rabi splitting of the levels) is relatively weak. Therefore the condition imposed by Eq. (12) may be poorly fulfilled and nonadiabatic transfer to the other dressed states may lead to a substantial loss of population. For optimum delay, the mixing angle should reach an angle of $\pi/4$ when Ω_{eff} reaches its maximum value.

C. Considerations for pulsed lasers

When pulsed laser radiation is involved, it is more convenient to square both sides of Eq. (14) and obtain the constraint

$$\Omega_{eff}^2 \Delta\tau > \frac{100}{\Delta\tau}. \tag{15}$$

The left-hand side of this equation is proportional to the pulse energy. For an atomic or molecular state with a typical radiative lifetime of the intermediate state $|2\rangle$ of the order of 100 ns, and a laser pulse width of 5 ns (typical for Nd-YAG lasers), Eq. (15) is satisfied for pulse energies of the order of 0.1 to 1 mJ.

The equations given above are valid for coherent radiation with transform-limited bandwidth, i.e., with negligible phase fluctuations during the interaction period.[3] When the bandwidth $\Delta\nu$ of the laser is small compared to $\Delta\tau^{-1}$ (for cw lasers we have typically $\Delta\nu = 1$ MHz and $\Delta\tau = 100$ ns), neglect of phase fluctuations is well justified. Pulsed lasers, however, have inferior coherence properties. A careful study of the effect of phase fluctuations on the transfer efficiency (Kuhn *et al.*, 1992) shows that Eq. (15) needs to be modified and should read

$$\Omega_{eff}^2 \Delta\tau > \frac{100}{\Delta\tau}\left[1 + \left(\frac{\Delta\omega_L}{\Delta\omega_{TL}}\right)^2\right]\Gamma, \tag{16}$$

where the last term in the bracket is the ratio of the actual laser bandwidth ($\Delta\omega_L$) to the transform-limited bandwidth for the given pulse length ($\Delta\omega_{TL}$). The factor Γ depends on the spectral profile (e.g., Gaussian or Lorentzian) and is of the order of unity. In the time domain, phase fluctuations correspond to changes of the frequency. Therefore phase fluctuations of the pump and Stokes radiation, which are usually uncorrelated, lead to a time-dependent detuning from the two-photon resonance. Deviation from the two-photon resonance is detrimental to the formation of the trapped state, and losses due to nonadiabatic coupling will occur. For lasers that are not designed to yield close to transform-limited pulses, the ratio of the bandwidth in Eq. (16) often exceeds 30. When such lasers are used, typically a pulse energy exceeding 1 J would be needed to satisfy Eq. (16).

With reference to Eq. (15) or (16) we also note that, if a pulse energy of 1 mJ is adequate for adiabatic evolution during the transfer process when nanosecond pulses with transform-limited bandwidth are used, then a pulse energy of 1 J would be required to implement the process with laser pulses of picosecond duration. Therefore nanosecond lasers with (nearly) transform-limited bandwidth and a pulse energy of the order of 1 mJ are well adapted to implement the STIRAP process successfully. When lasers with ultrashort pulses are used, the rate of change of the mixing angle is too fast to guarantee adiabatic evolution at pulse energies that are typically available in the laboratory. However, coherent population transfer in an atomic system with tightly focused picosecond lasers has been demonstrated (Broers, van Linden van den Heuvell, and Noordam, 1992).

VI. MISCELLANEOUS

A. History of the problem and current activities

The process of coherent population transfer is closely connected to the formation of the trapped states [Eq. (8)]. Such states lead to dark resonances when the frequency of one laser is tuned to the two-photon resonance in a three-state system coupled by two radiation fields. Dark resonances were first observed and explained in 1976 (Arimondo and Orriols, 1976; Alzetta, Gozzini, Moi, and Orriols, 1976), but it was not until much later that they became more than a curious spectroscopic feature in experimental and theoretical work (see Arimondo, 1996).

The possibility that efficient population transfer might be induced by suitably delayed pulses was first recognized by Oreg, Hioe, and Eberly (1984) in theoretical work. Despite further theoretical analysis by Hioe (Hioe, 1983; Hioe and Eberly, 1984) this finding was essentially overlooked in the literature during the first years thereafter. In the attempt to find methods for efficient excitation of molecules to high vibrational states, the phenomenon was rediscovered in Kaiserslautern (Gaubatz *et al.*, 1988, 1990) while Hioe and Carrol had continued to examine the problem (Carroll and Hioe, 1987, 1989, 1990; Hioe and Carroll, 1988). The method was then quickly developed and applied to collision dynamics experiments (Dittmann *et al.*, 1992; Külz *et al.*, 1995). Among the interesting examples of analytic studies of adiabaticity in the STIRAP problem, we mention the recent work of Stenholm and collaborators (Laine and Stenholm, 1996; Vitanov and Stenholm, 1996). The work of Marte and Zoller (Marte, Zoller, and Hall, 1991) alerted scientists working in quantum optics and atom optics to the potential of this scheme, and the number of new experiments, suggested or executed,

[3]The theory of Fourier transforms places an upper bound $\Delta_{\omega TL} = 1/\tau$ on the bandwidth of a pulse whose duration is τ. Any fluctuations increase the bandwidth above this minimum value.

grew rapidly.[4] Theoretical and experimental work quickly went beyond the study of the basic properties and features of the three-state system (see the Appendices). Most of the work has been done with continuous lasers, but experiments with pulsed lasers have also been reported (see, for example, Sec. VI.B).

B. Relation to other coherent phenomena

It should be noted that the formation of a trapped state has application to a variety of phenomena induced by coherent radiation, such as electromagnetically induced transparency Harris, Field, and Imamoglu, 1990; Boller, Imamoglu, and Harris, 1991; Harris, 1993, 1997; Kasapi *et al.*, 1995), induced refractive index changes (Scully, 1991; Fleischhauer *et al.*, 1992; Harris, 1994), and lasing without inversion (Scully, Zhu, and Gavrielides, 1989; Scully and Fleischhauer, 1994; Lukin *et al.*, 1996; Padmabandu *et al.*, 1996).

It is instructive to comment briefly on the relation of the STIRAP process to phenomena such as electromagnetically induced transparency. For example, in the work of Harris and co-workers (Boller *et al.*, 1991; Harris, 1997), it was shown that a strongly absorbing vapor can be made transparent for the pump laser radiation, when a concurrent Stokes laser is sent through the vapor, if the coupling scheme is of the type shown in Fig. 1. As it turned out, if the Stokes laser is not sent into the vapor slightly ahead of the pump laser, the envelope of the latter lags behind the former as the pulses propagate through the medium.

The sequence of delayed pulse interactions is considered to be ''counterintuitive'' by those using it for population transfer (see Shore, 1995). This is an appropriate choice since a method for population transfer already widely and successfully used prior to the advent of STIRAP is the stimulated emission pumping technique mentioned in Sec. III. A (Dai and Field, 1994). For this method the sequence of interactions is ''intuitive'' since some of the population of state $|1\rangle$ is first transferred to the intermediate state before interaction with the Stokes laser stimulates some of that population to the final state.

Harris maintains (Harris, 1997) that the sequence of interactions in which the Stokes laser pulse precedes the pump laser pulse (by a time less than the pulse width) is the ''intuitive'' one. From the perspective of laser-induced transparency this is indeed correct. The Stokes laser, which couples unpopulated states, is initially not absorbed. However, the strong coherent interaction leads to a dynamic Stark splitting of the levels. Interference of the transition amplitudes from state $|1\rangle$ to these two components (of what was initially the bare state $|2\rangle$ but becomes a coherent superposition of states $|2\rangle$ and $|3\rangle$ when the Stokes pulse acts) results in a cancellation

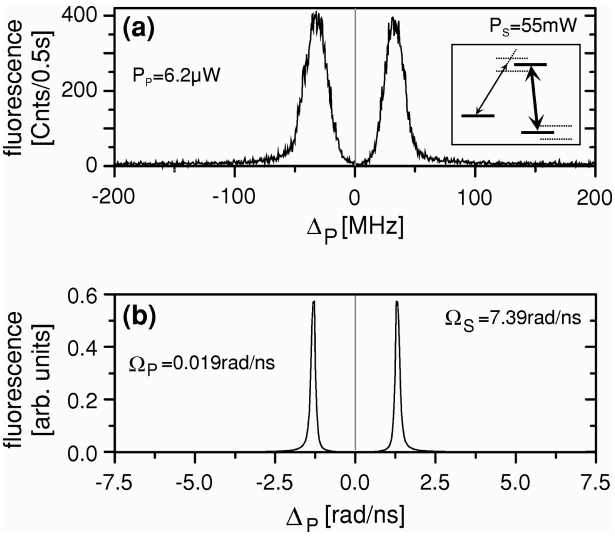

FIG. 10. The Autler-Townes splitting: (a) Experimental demonstration of the Autler-Townes splitting, induced by a strong Stokes radiation field (55 mW in a beam with FWHM of 0.5 mm) and probed by a weak pump laser. From this splitting, the Rabi frequency can be determined precisely. (b) Results of a numerical simulation of the splitting. As a consequence of interference of the transition amplitude to the two Autler-Townes components, the intensity goes to zero in the middle between the peaks.

of the absorption for those frequencies that were originally in resonance with the transition from state $|1\rangle$ to state $|2\rangle$. Obviously, the Stokes laser pulse ''clears the way'' for the pump laser pulse and therefore must lead the latter through the vapor.

An example is shown in Fig. 10. For this experiment a strong Stokes pulse is applied at the appropriate resonance frequency of the bare atom. The interaction of this field with the atom produces a pair of ''dressed'' states whose energies are separated by the Rabi frequency. This energy separation (the Autler-Townes splitting; Shore, 1990, Sec. 10.4) is revealed when a weak probe pulse scans the frequency of a transition linked to either of the dressed states.

In STIRAP, it is exactly this same mechanism that prevents the pump laser from putting population into the intermediate state when the Stokes laser creates a large enough dynamic Stark splitting to eliminate the absorption of photons from the pump laser pulse. In the context of coherent population transfer, usually low-density vapor (such as is typical for molecular beams) is used and one is not concerned about propagation phenomena.

In summary, whether the delayed sequence of interactions typical for the STIRAP process is ''intuitive'' or ''counterintuitive'' depends on the perspective determined by the process under study.

C. Some remarks about ladder systems

In the preceding sections, we discussed the delayed interaction of two pulses with states in the lambda-type

[4]Kasevich and Chu, 1991; Broers *et al.*, 1992; Parkins *et al.*, 1993; Pillet *et al.*, 1993; Goldner *et al.*, 1994a, 1994b; Lawall *et al.*, 1996; Walser *et al.*, 1996; Kulin *et al.*, 1997a, 1997b.

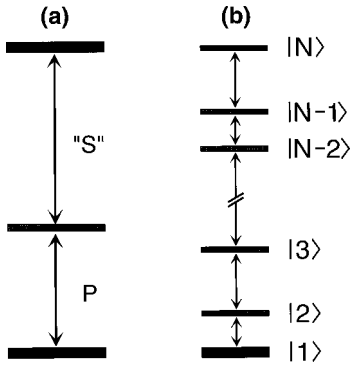

FIG. 11. A three-level ladder system and a multilevel chain of N levels connected by $N-1$ lasers.

configuration (see Fig. 1). All the discussion remains true for a ladder system (Shore *et al.*, 1991), wherein the final-state energy lies higher than that of the intermediate state (see Fig. 11). Indeed, transfer to high-lying electronic states of atoms has been successfully demonstrated (Broers *et al.*, 1992; Lindinger, Verbeek, and Rubahn, 1997; Süptitz, Duncan, and Gould, 1997). The transfer process needs to be completed, however, on a time scale short compared to the lifetime of the final state. Since Rydberg levels of atoms have lifetimes that are often of the order of μs or even longer, it is straightforward to implement the transfer process with pulsed radiation sources.

As discussed by Shore *et al.* (1992) and demonstrated by Noordam *et al.* (Broers *et al.*, 1992), ladder systems offer an alternative way of implementing the delayed sequence of interactions. The latter authors use a short pulse laser that carries enough bandwidth to be chirped across the transition frequency of both the $|1\rangle$-$|2\rangle$ and the $|2\rangle$-$|3\rangle$ pairs of states. When the frequency chirp is imposed such that states $|2\rangle$ and $|3\rangle$ are radiatively coupled somewhat earlier than states $|1\rangle$ and $|2\rangle$, efficient population transfer, with very little population ever residing in state $|2\rangle$, can be demonstrated.

Several generalizations of the three-state (lambda or ladder) systems have been considered or demonstrated (see also Appendix C). Efficient population transfer is possible from the first to the last state in an N-state system, coupled by $N-1$ radiation fields (Shore *et al.*, 1991; Oreg *et al.*, 1992), if the Stokes interaction with the pairs $|N\rangle$-$|N-1\rangle$, $|N-2\rangle$-$|N-3\rangle, \ldots,$ $|3\rangle$-$|2\rangle$ begins earlier than the pump interaction with the pairs $|1\rangle$-$|2\rangle$, $|3\rangle$-$|4\rangle, \ldots,$ $|N-2\rangle$-$|N-1\rangle$. Each of the Stokes interactions may coincide in time, as may the pump interactions. There is little if any transient population into states $|2\rangle$, $|4\rangle, \ldots,$ while some transient population is found in states $|3\rangle, |5\rangle, \ldots$. If the coherence in the system is not disturbed during the interaction, either by collisions or radiative decay, then all of the population reaches the final state.

Several authors have described multilevel excitation schemes that supplement the pump and Stokes pulses with longer interactions (Smit, 1992; Hioe and Carroll, 1996). Based on numerical results using local optimization theory, (Malinovsky and Tannor, 1997) have very recently suggested that the efficiency of population transfer in N-state systems, $N>3$, can be increased if the (Stokes) interaction is first between states $|N\rangle$ and $|N-1\rangle$, followed by the (pump) interaction between states $|1\rangle$ and $|2\rangle$, and during both of these interactions there is an interaction that couples the other states. With such a scheme there can be very little transient population not only in states $|2\rangle,|4\rangle,\ldots,|N-1\rangle$ but also in states $|3\rangle, |5\rangle, \ldots, |N-2\rangle$. Therefore the process will be more robust against radiative decay of these intermediate states. It would be interesting to verify these findings experimentally. Such experiments are in preparation in Kaiserslautern.

For completeness we mention the Raman chirped adiabatic passage (RCAP) method as a different ladder-climbing technique (Chelkowski and Gibson, 1995); Chelkowski and Bandrauk, 1997; Guerin, 1997). Implementation of the RCAP technique requires a coherent short laser pulse with sufficient bandwidth to cover the change in transition frequency between the lowermost and the uppermost pairs of states. If the chirp is conducted such that the frequency sweeps initially across the $|1\rangle$–$|2\rangle$ transition, and finally across the $|N-1\rangle$–$|N\rangle$ transition then population is driven from state $|1\rangle$ to state $|N\rangle$ in a sequence of adiabatic passage processes between adjacent states, from the lower to the upper state.

VII. SUMMARY

We have sketched the theory underlying the STIRAP process, whereby pairs of partially overlapping pulses produce complete population transfer. The procedure is remarkable for its relative insensitivity to details of the pulses (e.g., precise shape of the pulse envelope or pulse fluence). In the Appendices we have noted the connection between the STIRAP mechanism and various coherence effects in pulse propagation, and we have also noted some applications in quantum optics and atom optics.

Like any two-photon or Raman process, the method allows excitation transfer between states for which a single-photon transition is forbidden (e.g., by parity). In particular, it can be used to transfer population between fine-structure levels or magnetic sublevels. Whereas the main text of this article discusses the essential, basic principles of STIRAP, the Appendices present further examples and extensions.

In Appendix A, we present more details of examples in which the simple theory of three-state STIRAP has been extended to treat multiple levels.

In Appendix B, we discuss a variety of experimental implementations of the STIRAP scheme, to atoms, diatomic molecules, and triatomic molecules. It should be noted that, although studies of coherent excitation rely almost entirely upon the collisionless environment of an atomic or molecular beam, the STIRAP process has also been demonstrated using a vapor cell (Kuhn, Steuerwald, and Bergmann, 1998).

In Appendix C, we discuss ways in which the STIRAP process, used to transfer population between magnetic sublevels, can be used to impart transverse momentum to an atomic beam, thereby inducing beam deflection. The robustness of the STIRAP mechanism is particularly useful for such applications, as can be seen in the coherence properties of the prepared state.

In Appendix D, we comment on an area of application for STIRAP which is currently being explored, whereby a continuum (ionization or dissociation) serves as the intermediary for the Raman process.

ACKNOWLEDGMENTS

The work of B.W.S. was supported in part under the auspices of the U.S. Department of Energy at Lawrence Livermore National Laboratory under contract W-7405-Eng-48 and in part by an Alexander von Humboldt Foundation Research Award. We gratefully acknowledge a NATO Collaborative Research Grant, support by the Deutsche Forschungsgemeinschaft, and partial support by the EU network "Laser-Controlled Dynamics of Molecular Processes and Applications," ERB-CH3-XCT-94-0603.

APPENDIX A: COHERENT POPULATION TRANSFER IN MULTILEVEL SYSTEMS

1. Setting up multilevel systems

In the main text we have considered the radiative interaction of delayed pulses with a system of three isolated (and nondegenerate) states. Although this is justified in some cases, the multilevel nature of the energy-level structure needs to be taken into account in most other cases. Level splitting (due to fine structure, hyperfine interaction, Zeeman splitting, or a high level density in a polyatomic molecule) may invalidate the assumption that the lasers interact with only one pair of levels. As we shall see, the consequences of nearby degenerate states in the final state (only one of which will be in exact two-photon resonance with the initial state) may be particularly important and possibly detrimental.

The Ne* atom has proven very convenient for the study of coherent population transfer in multilevel systems, since a magnetic field may be used to remove the degeneracy of the magnetic sublevels in the intermediate and final levels. Furthermore, optical selection rules can be invoked to control the number of levels that participate in the process, as shown in Fig. 12. The quantization axis is set by the direction of a uniform magnetic field **B**. When the direction of linear polarization of both the pump and the Stokes laser is chosen parallel to **B**, the selection rule $\Delta m=0$ applies, and only three states with $m=0$, one each in the initial, intermediate, and final level, are coupled by the radiation. When the Stokes or pump laser polarization is perpendicular to **B** while the other laser remains polarized parallel to it, four or five levels, respectively, are involved in the process [see Fig. 12(b) and 12(c)]. When neither the Stokes laser nor the pump laser polarization is parallel or perpendicular to the direction of the **B** field all nine sublevels are coupled [Fig. 12(d)].

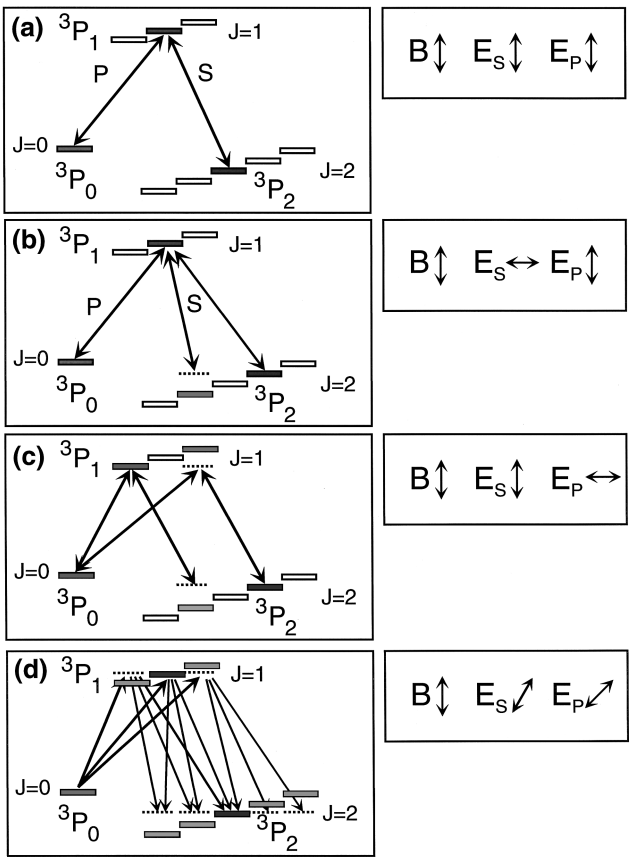

FIG. 12. Various linkages in a three-level system with Zeeman splitting of the sublevels. The coupling scheme is controlled by the polarization of the pump and Stokes laser radiation with respect to the magnetic field **B**.

2. Experimental results

For further reference, Fig. 13 shows the population transfer when only three states are coupled. The frequency of the Stokes laser is varied in steps while the frequency of the pump laser is tuned across the resonance. The data shown in Fig. 8(a) are equivalent to one trace of those given in Fig. 13. The broad feature results from population transfer to the final state by spontaneous emission induced by the pump laser, while the narrow feature is related to coherent population transfer. When the Stokes laser is, for instance, tuned about 200 MHz off resonance, the STIRAP transfer occurs when the pump laser is also tuned off resonance by about 200 MHz. Thus the narrow spikes track the two-photon resonance. A high transfer efficiency is observed for detuning as large as 300 MHz off the resonance with the intermediate level. The transfer efficiency at two-photon resonance does not change within the range of detuning shown in the figure. However, the width of the two-photon resonance increases as the frequencies are tuned close to the one-photon resonance.

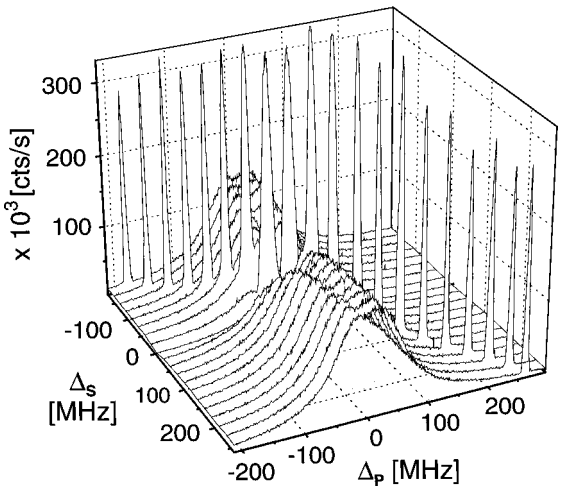

FIG. 13. Coherent population transfer from the $^3P_0$ to the $^3P_2$ level of Ne* for a three-level system [see Fig. 12(a)] as a function of the Stokes and pump laser detuning Δ_S and Δ_P. The "STIRAP ridge" along the line, for which the two-photon resonance $\Delta_S=\Delta_P$ is maintained, is clearly seen.

Rotation of the Stokes and pump laser polarization to angles other than 0° or 90° (resulting in the coupling of all sublevels) leads to dramatically different results (see Fig. 14). The line that tracks the two-photon resonance is again apparent. Along this line, the condition for adiabatic evolution given by Eqs. (12), (13), or (14) is fulfilled. Nevertheless, three notches in the ridge are apparent where transfer fails. A more detailed discussion of these observations can be found in Martin, Shore, and Bergmann (1996). In the next section we analyze the problems that may occur for coherent population transfer in multilevel systems using a specific example.

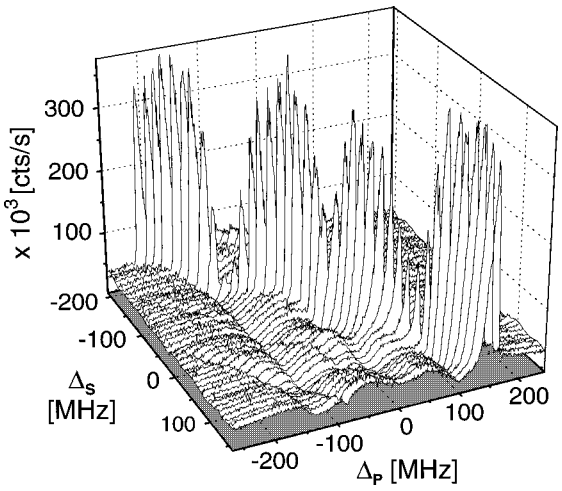

FIG. 14. Coherent population transfer from the $^3P_0$ to the $^3P_2$ level for Ne* for a multilevel system [see Fig. 12(d)] as a function of the Stokes and pump laser detuning Δ_S and Δ_P. The "STIRAP ridge" along the line, for which the two-photon resonance $\Delta_S=\Delta_P$ is maintained, is clearly visible. Along this line, the condition displayed by 14 is fulfilled. Nevertheless, there are notches in the ridge where transfer fails. In these regions, crossings of dressed-state eigenvalues may block the path for adiabatic transfer.

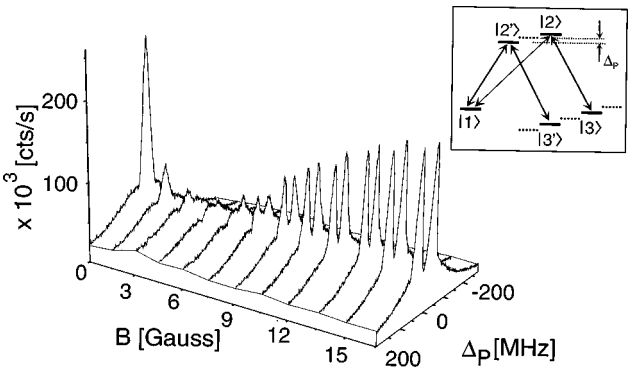

FIG. 15. Coherent population transfer from the $^3P_0$ to the $^3P_2$ level of Ne* for a linkage scheme shown in Fig. 12(c) (five-level system), as a function of the magnetic field which determines the magnetic sublevel splitting. Efficient transfer is possible for zero and large magnetic fields. Transfer fails for small B fields because the adiabatic transfer path is blocked.

3. A specific case: Dependence of the transfer efficiency on magnetic-field strength

Figure 15 shows the variation of the transfer efficiency for a combination of polarizations which lead to the coupling of five states. The Stokes laser frequency is held fixed, tuned to resonance with one of the intermediate states, while the pump laser frequency is tuned across the one- and two-photon resonance and the magnetic field is changed in increments. For $|\mathbf{B}|=0$, when the m sublevels in the intermediate and final states are degenerate, a high transfer efficiency is observed. Transfer occurs to both of the degenerate magnetic sublevels $m=+1$ and $m=-1$. When the magnetic-field strength is increased to about 3 G, coherent population transfer does not occur. However, as the field strength increases farther, a high transfer efficiency is recovered, which now occurs to either $m=-1$ or $m=+1$, depending on which sublevel is in two-photon resonance. (It is interesting to note that Fig. 15 also demonstrates the possibility of orienting the atomic angular momentum, simply by tuning the frequency of a laser to the respective two-photon resonance.)

The reason for the success of population transfer at zero and large magnetic fields but its failure at some intermediate values can be understood by considering the evolution of the energies of dressed eigenstates, as shown in Fig. 16. With five bare states coupled by the coherent radiation fields we also have five dressed eigenstates. The variation of their eigenvalues with time is shown in the figure. For $|\mathbf{B}|=0$, the pattern appears similar to the one for only three states. Since the frequencies are tuned to the one-photon and two-photon resonances with the degenerate intermediate and final states, respectively, the five eigenvalues are degenerate at early and at late times [Fig. 16(a)]. As in the case of three states [Fig. 3(c)], we have a zero-energy eigenvalue at all times, i.e., we have an adiabatic path that connects the zero-energy dressed-state eigenvalue at early times when the pump laser is not yet turned on (and which relates to the bare state $|1\rangle$ which carries the

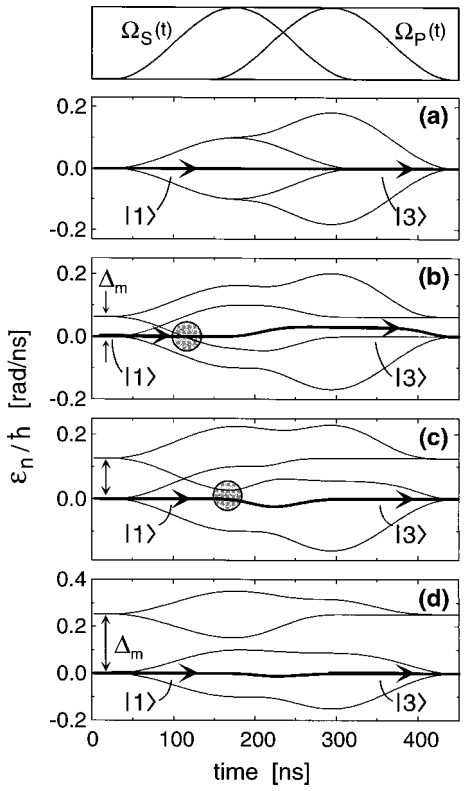

FIG. 16. Variation of the dressed-state eigenvalues with time and for various magnetic fields. The splitting of the doubly or triply degenerate states at $t=0$ gives the Zeeman splitting of the magnetic sublevels in the final level. The circles mark the crossing of dressed-state eigenvalues, which determines whether the adiabatic transfer path is blocked or not.

population initally) and the zero-energy eigenvalue at late times, when the Stokes laser has been turned off (and which is related to the bare state $|3\rangle$, supposed to receive all the population at later times). Thus coherent population transfer is possible, as verified in the experiment (Fig. 15).

When the **B** field is not zero, Zeeman splitting removes the m-sublevel degeneracy. Two-photon resonance is established between the initial state and only one of the final states. As a consequence, the dressed-state eigenvalues are no longer degenerate at early and late times. (We have assumed that the Zeeman splitting in the intermediate and final states is the same and that the laser frequencies are in resonance with one of the intermediate states.) Therefore, at early times, we have a triple degeneracy, which is lifted as soon as the Rabi frequency of the Stokes laser is nonzero, and a double degeneracy of states, separated from the former ones by the detuning from the two-photon resonance, i.e., by the Zeeman splitting. The triplet is associated with the three bare states that are resonantly coupled by the radiation field, while the doublet is associated with the other two. These latter states also show a Rabi splitting, and, since at early times their energy is separated from that of the other three states, a crossing of the states occurs, provided the Rabi frequency exceeds the Zeeman detuning.

Further analysis shows that a coupling between states, related to the energy levels that cross, is induced by the pump laser. When the splitting is small (because the magnetic field is small), this crossing occurs before the pump laser is turned on, and the system, which initially evolves along the zero-energy path, passes (diabatically) through this crossing. At intermediate times, however, the pump laser induces interactions between the states and forces the energy of the transfer path to deviate from zero. At later times, the transfer path does not connect to the state with zero energy when the Stokes laser is turned off, as needed for successful completion of the transfer. Therefore the adiabatic transfer path is blocked and coherent population transfer is not possible [Fig. 16(b)].

With increasing magnetic-field strength, leading to larger Zeeman splitting, the curve crossing with the zero-energy path occurs later, after the pump laser is turned on [Fig. 16(c)]. Since the pump laser couples the related dressed states, an avoided crossing develops. Although a transient deviation from zero energy is observed (meaning that some atoms will transiently reside in one of the intermediate states and may be lost by radiative decay), the transfer path connects to the zero-energy eigenvalue as the Stokes laser is turned off. Population transfer is again possible. At even larger Zeeman splitting, the avoided crossing is barely visible and a (nearly) zero-energy transfer path is again established [Fig. 16(d)]. In this latter case, the Zeeman splitting in the intermediate and final states is larger than the Rabi frequency. Therefore the relevant bare states can again be considered as a (nearly) isolated three-state system.

Interaction of the states and the related crossing of their eigenvalues, as discussed above, is also responsible for the failure of the transfer at certain detunings from the intermediate resonance, shown in Fig. 14. The notch in the center of the STIRAP ridge is a consequence of a temporary deviation of the adiabatic transfer path from zero energy [similar to the situation shown in Fig. 16(c)], which otherwise connects to the appropriate states at early and late times. The other two notches are due to the blocking of the adiabatic transfer path [similar to the situation shown on Fig. 16(b)].

It is important to note that the failure of the transfer at small magnetic fields can be cured, for instance, by tuning the laser frequencies somewhat off the resonance with any one of the intermediate states [see Fig. 17(a), to be contrasted with the on-resonance case shown in Fig. 15]. Figure 17(b) shows an example from Martin *et al.* (1996) in which population transfer is possible for small Rabi frequencies but failure due to the blocking of the adiabatic path occurs at higher laser power. The efficiency and robustness of population transfer in a three-state system increases with increasing Rabi frequency. This is obviously no longer true, at least not in general, in a multilevel system.

In summary, coherent population transfer in multilevel systems depends on the availability of an adiabatic path that connects the initial and final states with only a small deviation from the zero eigenvalue at intermediate

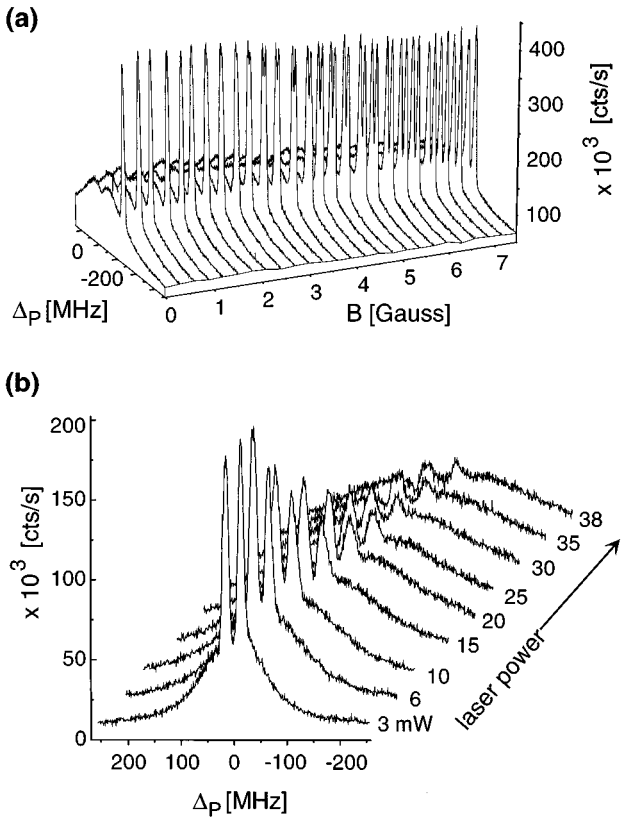

FIG. 17. Coherent population transfer from the $^3P_0$ to the $^3P_2$ level of Ne*. The results shown in (a) refer to the same linkage pattern as in Fig. 15, except for detuning $\Delta_S=200$ MHz of the laser frequencies from resonance with the intermediate level. This detuning prevents the detrimental crossing of dressed-state eigenvalues (see Fig. 16) and a blocking of the adiabatic transfer path does not occur (Martin *et al.*, 1996, Fig. 15). In (b) we see an example of decreasing efficiency of population transfer with increasing Rabi frequency. The magnetic-field strength here is 7.5 G [Martin *et al.*, 1996, Fig. 20(b)].

times when both laser fields are nonzero. Whether this is possible or not depends on the level structure and coupling scheme. In most cases, an analysis like the one shown in Fig. 16 is needed in order to understand the details of the transfer process and to make an appropriate choice of Rabi frequencies and detunings in order to control the crossing of dressed-state eigenvalues.

APPENDIX B: SOME RESULTS FOR PULSED LASER EXCITATION

1. General remarks

A particularly interesting application of the STIRAP process is the selective excitation of molecules to high-lying vibrational levels. In fact, the attempt to achieve this goal was the initial motivation for the development of this scheme (Gaubatz *et al.*, 1990). Most molecules have their first accessible electronic state at energies exceeding 3 eV. Therefore radiation in the ultraviolet spectral region is required to couple, for instance, the vibrational ground level to a high vibrational level in a

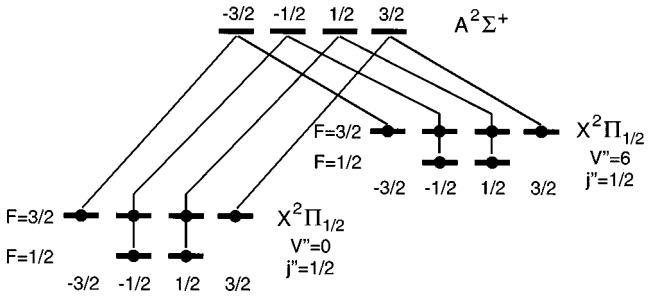

FIG. 18. The relevant energy-level scheme for coherent population transfer in the NO molecule with the linear polarization of the pump and Stokes laser radiation, polarized parallel to each other. With hyperfine levels included, a total of 18 states are coupled. The numbers 1/2 and 3/2 give the m_F quantum numbers, unless specified otherwise.

Raman-type linkage. Since the relevant transition dipole moments are typically smaller than for atoms, the adiabaticity requirement [Eq. (15)] cannot be satisfied with radiation from cw lasers. Pulsed sources need to be used. Pulsed lasers have, however, inferior coherence properties, and so the consequences of Eq. (16) must be considered. Numerical evaluation of Eq. (16) for laser pulses with energies of the order of mJ, pulse lengths of the order of a few ns, and electronic lifetimes of the intermediate state of the order of 100 ns shows that nearly transform-limited radiation is needed to guarantee adiabatic evolution during the transfer process (Kuhn *et al.*, 1992). Large deviation from a transform-limited bandwidth is indicative of strong phase fluctuations or a large frequency chirp, which are detrimental to the process of coherent population transfer. To generate suitable radiation, one typically starts from single-mode cw radiation, which is then pulse amplified and subsequently frequency doubled or mixed as needed (Schiemann *et al.*, 1993). In the following we discuss briefly some results obtained for the NO and the SO_2 molecules. The former serve as an example of complications that may possibly arise because of the hyperfine interaction, while the latter are an example of STIRAP for a polyatomic molecule.

2. The NO molecule

The relevant energy-level structure for the NO molecule is shown in Fig. 18. The molecule has a $^2\Pi_{1/2}$ electronic ground state, and lambda-doubling (Herzberg, 1950) is observed. Only levels with different parity are radiatively coupled. What seems to be a three-state system see (Fig. 18) is actually a system of 18 states. Because $^{14}N^{16}O$ has a nuclear spin of $I=1$, each of the three levels has a total angular momentum of $F=1/2$ and 3/2 and, in turn, magnetic quantum number $|m_F|=1/2$ and 3/2. Such hyperfine splitting could be detrimental to efficient population transfer (as discussed in Sec. A for the case of Zeeman splitting), because coupling may also occur to states which are not in two-photon resonance. However, for linear polarization, and when $\mathbf{E}_P$ is parallel to $\mathbf{E}_S$, the 18-state system decomposes into two in-

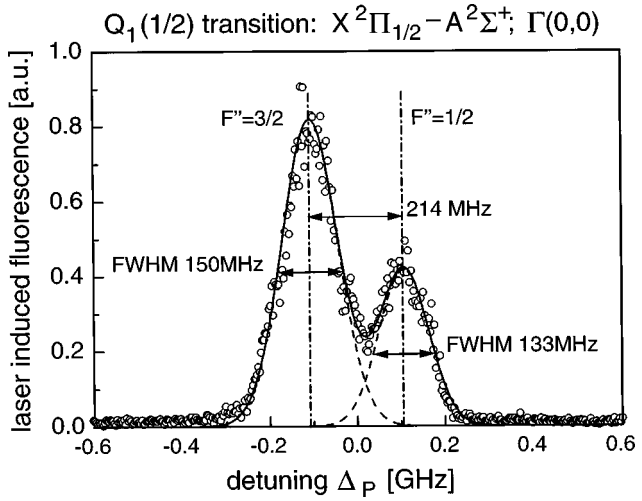

FIG. 19. Laser-induced fluorescence as the pump laser is tuned across the resonance with the level in the A state. The hyperfine splitting of 214 MHz in the ground state is resolved. The difference in width between the smaller and larger peak (17 MHz) is related to the hyperfine splitting of the upper state. This figure also confirms that the bandwidth of the laser does not exceed 130 MHz.

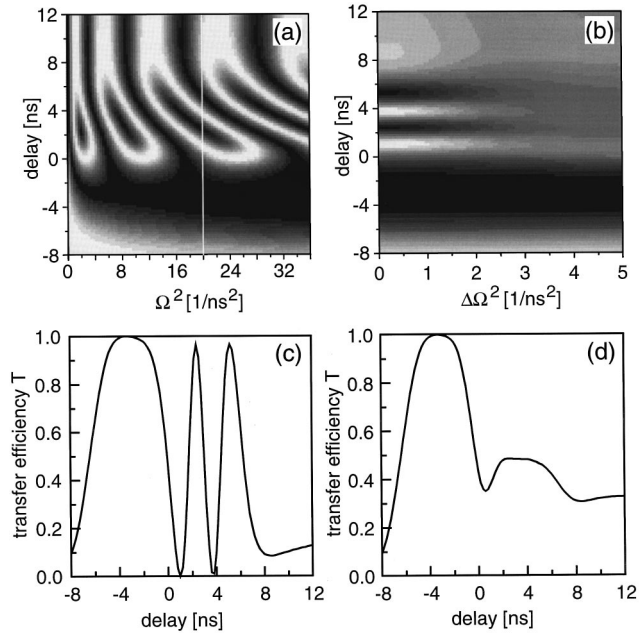

FIG. 20. Efficiency of coherent population transfer (numerical results for NO) as a function of the Rabi frequency and time delay. The Rabi frequencies related to the pump and Stokes laser are equal. Black areas (upper two panels) indicate efficient transfer; white areas are those where transfer fails. The large plateau shows where the transfer efficiency is insensitive to small variations of the time delay and the Rabi frequencies. Results averaged over a large number of pulses are shown (a) with no pulse-to-pulse fluctuations of the energy per pulse and (b) with Gaussian-distributed fluctuations with a standard deviation of up to $\Delta(\Omega^2)=5\times10^{18}$ s^{-2} (units) around a mean value of $\Omega^2=20\times10^{18}$ s^{-2}, see dashed line in Fig. 20(a). The left and right lower panels show the transfer efficiency T explicitly for $\Omega^2=20\times10^{18}$ s^{-2} for $\Delta\Omega=0$ and 5×10^{18} s^{-2}, respectively. The latter reveals the characteristic variation of T with the delay (the STIRAP signature) for pulsed lasers. 10% fluctuations (Gaussian-distributed).

dependent three-state systems ($F=3/2$ and $m_F=+3/2$ or $-3/2$) and two six-state systems for $m_F=+1/2$ and $-1/2$. The hyperfine splitting of the intermediate level (the electronic A state) is 15 MHz (Feller *et al.*, 1993) and cannot be resolved with pulsed lasers of a few ns duration, while the splitting of the initial and final levels is 214 MHz (Miller and Feller, 1994). This latter splitting is large enough to be fully resolved in this experiment (see Fig. 19), so the complexity of the level system is further reduced. Depending on the exact value of the frequency, difference of the pump and Stokes laser transfer between the states with $m_F=1/2$ may occur between the $F=1/2$ levels in parallel with transfer between the $F=3/2$ levels, or from $F=1/2$ (3/2) to $F=3/2$ (1/2). Because the hyperfine splitting is just large enough to exceed the transform-limited linewidth of the laser, there is always only a single final quantum state that is in two-photon resonance with the initial state. In this case, the crossing of dressed-state eigenvalues, which could be detrimental, does not occur (Kuhn *et al.*, 1998).

Numerical modeling results, exhibiting a clear "STIRAP signature," are shown in Fig. 20(a). The plots show the transfer efficiency (white: large transfer efficiency; dark: no transfer) as a function of the pulse delay and the Rabi frequency, for the special case when Ω_P and Ω_S have equal maximum value. When the delay is negative (Stokes before pump), the plateau region, where the transfer is insensitive to small changes of the delay (see also Fig. 9), is clearly developed. The plateau broadens as the Rabi frequency is increased. For overlapping pulses (zero delay) Rabi oscillations occur. Whether transfer to the final state is possible or not depends on the exact value of the pulse area (see Sec. II) of the laser pulses. Therefore the transfer efficiency varies between zero and unity as the Rabi frequency changes. When the delay is positive (the pump pulse precedes the Stokes pulse) and large, the pump laser induces Rabi oscillations between levels $|1\rangle$ and $|2\rangle$. For a pump pulse area $A_P=(2n+1)\pi$, all population resides in level $|2\rangle$ at the end of the pump pulse and Rabi cycling of the population between states $|2\rangle$, driven by the Stokes lasers, begins. Since, for the special case shown in Fig. 20, the pulse areas of both lasers are equal, all population will be found in state $|3\rangle$ at the end of the Stokes laser pulse, independent of the pulse delay. When the delay is positive but the laser pulses overlap, the transfer efficiency to level $|3\rangle$ does depend on the time delay.

Since the pulse energy of pulsed lasers fluctuates, often as much as 10%, the average transfer efficiency can be obtained from data such as those shown in Fig. 20(a) by averaging over the appropriate range of Rabi frequencies. It is obvious that these fluctuations do not affect the transfer efficiency in the region of the plateau

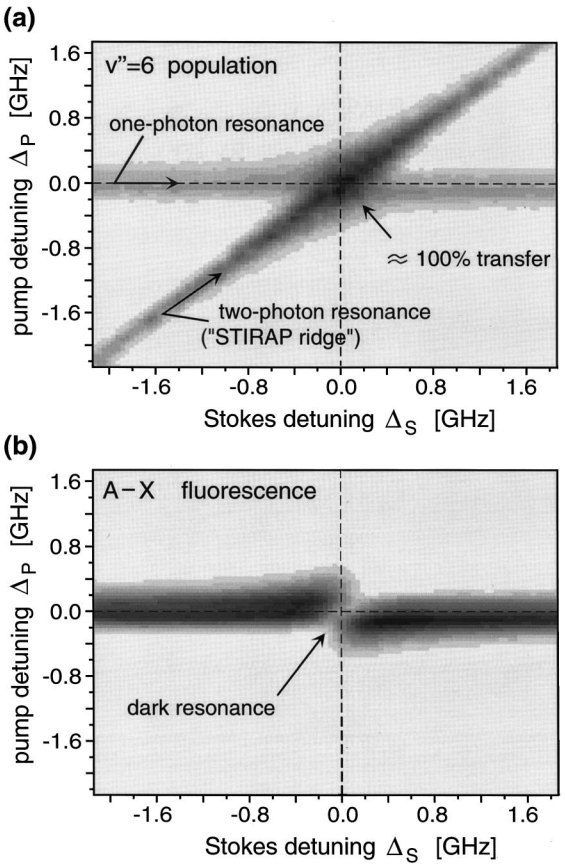

FIG. 21. Coherent population transfer and dark resonance for the NO molecule as a function of the pump and Stokes laser detuning. Population of the final level (equivalent to the result for Ne*; see Fig. 12) is shown in (a) while the fluorescence from the intermediate level is shown in (b). Dark areas are those where a large signal is observed.

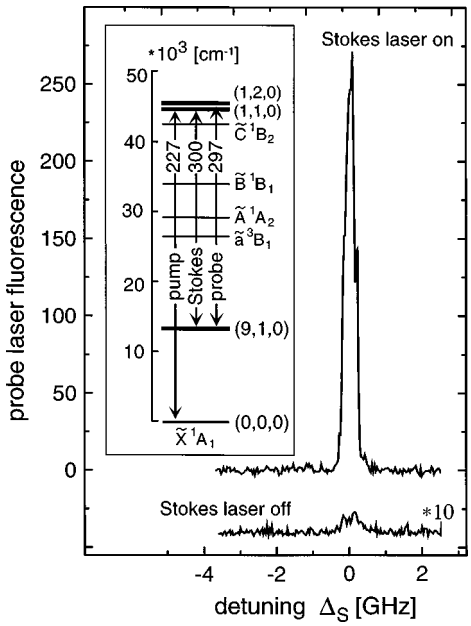

FIG. 22. Coherent population transfer in the SO_2 molecule. The level diagram is also shown. The lower trace, with the Stokes laser turned off, has been multiplied by a factor of 10. In this case, the fluorescence reaches the final level by spontaneous emission from the intermediate one. When the Stokes laser is on (and the conditions for efficient transfer are met), the population of the final level increases by more than two orders of magnitude.

(negative delay), but the transfer efficiency for zero or positive delay depends on the actual value of the mean Rabi frequency as well as on the extent of the fluctuations [as measured by the standard deviation $\Delta(\Omega^2)$ from the mean value $\langle\Omega^2\rangle$]. The transfer efficiency after such an averaging is shown in Fig. 20(b). The data of Fig. 20(b) refer to $\langle\Omega^2\rangle = 20\times10^{18}\ \mathrm{s}^{-2}$, as marked by the white line in Fig. 20(a). The transfer efficiency T shown in Fig. 20(b) for $\Delta(\Omega^2) = 20\times10^{18}\ \mathrm{s}^{-2}$ is identical to the one along the dashed line in Fig. 20(a). That variation of T with the delay is also shown explicitly in Fig. 20(c). As the standard deviation increases from 0 to $5\times10^{18}\ \mathrm{s}^{-2}$, the oscillatory dependence of T on the delay is damped. The transfer efficiency for $\Delta(\Omega^2) = 5\times10^{18}\ \mathrm{s}^{-2}$ is shown explicitly in Fig. 20(d). This plot reveals the STIRAP signature of the transfer with pulsed lasers, as clearly observed by Schiemann *et al.* (1993) and Halfmann and Bergmann (1996).

Finally, the transfer efficiency as a function of the detuning of both lasers is shown in Fig. 21(a) (equivalent to Fig. 13 for transfer with a cw laser). High transfer is observed along the two-photon resonance, the broadening of which near the one-photon resonance is obvious. When the pump laser frequency is on one-photon resonance but the Stokes laser frequency is not, the former laser excites molecules to the intermediate state and some population reaches the final level by spontaneous emission. Figure 21(b) shows the fluorescence from the intermediate level, which is strong only for $\Delta_P \approx 0$. The dark resonance for $\Delta_P \approx \Delta_S \approx 0$ is also clearly visible.

3. The SO_2 molecule

The adiabatic following condition, Eq. (16), imposes a lower limit on the pulse energy required for efficient population transfer by the STIRAP process. The enormously increased density of levels in a polyatomic molecule, as compared to an atom or a diatomic molecule, typically results in a substantially smaller line strength of a particular transition. With adequate power, and when the density of levels in the final state is not too high, efficient transfer in a polyatomic molecule is possible. Figure 22 shows transfer from the $(J,K) = (3,3)$ level of the vibrational ground state $(0,0,0)$ to the same rotational levels of a high overtone $(9,1,0)$. Without the Stokes laser, some population reaches the final state by fluorescence from the intermediate level. The lower trace of Fig. 22(b) shows the probe laser-induced fluorescence from the final level, which needed to be multiplied by 10 in order to be seen on this scale. When the Stokes laser is on and appropriately timed, the population in the final level increases by more than two orders of magnitude. A transfer efficiency of nearly 100% has also been demonstrated in this case (Halfmann and Bergmann, 1996).

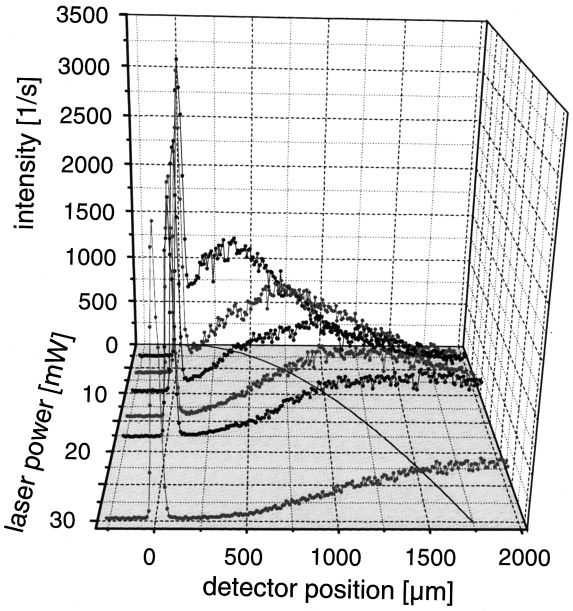

FIG. 23. Deflection of a metastable Ne* beam by the spontaneous emission force. Excitation occurs on the closed cycle $^3P_2 \leftrightarrow {}^3D_3$ transition. The narrow, tall peak gives the profile of the undeflected beam, marked here by the ^{22}Ne isotope, which is not excited. With increasing laser power (3, 6, 10, 15, 18, and 30 mW from back to front), the maximum of the broad peak moves farther away from the undeflected beam. The solid line on the base plane shows the predicted position of the mean deflection.

APPENDIX C: COHERENT MOMENTUM TRANSFER

1. Deflection by spontaneous emission forces

The process of coherent population transfer is also associated with the exchange of momenta between the radiation fields and the atom. Momentum transfer is a key process in atom optics, for instance, for the design of matter-wave mirrors and beam splitters. Because the STIRAP process eliminates spontaneous emission, it also holds promise for dissipation-free momentum transfer (Marte *et al.*, 1991).

To set the stage for our discussion, we show in Fig. 23 the deflection of a highly collimated Ne* beam by the spontaneous emission force. The frequency of the laser, which crosses the atomic beam at a right angle, is tuned to resonance with the closed-cycle 640-nm transition $^3P_2 \leftrightarrow {}^3D_3$ (see Fig. 6). A photon that is absorbed transfers not only its energy to the atom but also its momentum. The subsequent spontaneous emission of photons results in a recoil that is randomly distributed. The mean momentum transfer due to the recoil after N cycles of absorption and emission is zero, while the atom has accumulated a momentum of $N\hbar k$ in the direction of laser-beam propagation. The rate of absorption—emission cycles is limited by the spontaneous emission rate. In the limit of strong saturation, the number N of absorbed photons is given by $N=\Delta t/\tau_r$, where Δt is the interaction time with the laser and τ_r is the radiative lifetime. The dissipative nature of the emission process leads to a wide distribution of deflection angles.

Figure 23 gives examples. The intensity profile of a highly collimated atomic beam is recorded with a channeltron detector behind a 10-μm slit, which moves perpendicular to the atomic-beam axis. The narrow peak marks the position of the undeflected beam. It is related to the ^{22}Ne isotope, which does not participate in the absorption-emission cycles. The ^{20}Ne atoms in the $^3P_2$ state are deflected. The mean deflection angle as well as the width of the distribution increases with increasing power. The dissipative nature of this process inhibits the deflection of the majority of the atoms to a very narrow range of angles. It furthermore does not allow preservation of any coherence that may have been created in the matter wave. Momentum transfer induced by a STIRAP process overcomes these limitations.

2. Multiphoton coherent momentum transfer

In the following, we discuss momentum transfer via coherent population transfer within the $^3P_2$ magnetic sublevels induced by circularly polarized radiation, the frequency of which is tuned into resonance with the $^3D_2$ level. As shown in Fig. 24, two σ^+ photons and two σ^- photons couple the $m=-2$ and the $m=+2$ states. When the laser beams of different polarization propagate in opposite directions, the momentum transfers due to the absorption process (σ^+ light) and the stimulated emission process (σ^- light) are in the same direction.[5]

We now consider the question of whether it is possible to have a STIRAP process involving not only two but four photons (Shore *et al.*, 1991). A requirement is the existence of a dressed eigenstate with a zero-energy eigenvalue throughout the interaction (Hioe and Carroll, 1988). The Hamiltonian of this five-state system reads

$$\mathsf{H}(t)=\frac{\hbar}{2}\cdot\begin{bmatrix} 0 & \Omega_{12} & 0 & 0 & 0 \\ \Omega_{21} & 2\Delta_{12} & \Omega_{23'} & 0 & 0 \\ 0 & \Omega_{3'2} & 2\Delta_{13'} & \Omega_{3'2'} & 0 \\ 0 & 0 & \Omega_{2'3'} & 2\Delta_{12'} & \Omega_{2'3} \\ 0 & 0 & 0 & \Omega_{32'} & 2\Delta_{13} \end{bmatrix}. \tag{C1}$$

A solution of the eigenvalue equation

$$\mathsf{H}(t)\mathbf{C}=0 \tag{C2}$$

exists if the determinant vanishes at all times,

$$\det \mathsf{H}(t)=0. \tag{C3}$$

The determinant of Eq. (C3) can be rewritten in the form

[5]Discussing the process in terms of absorption and stimulated emission is illustrative but may be misleading. In the context of STIRAP, the stimulated process does not transfer population that resides in the intermediate level to the third level. Rather, the transfer occurs through a multiphoton process directly from the initially populated state.

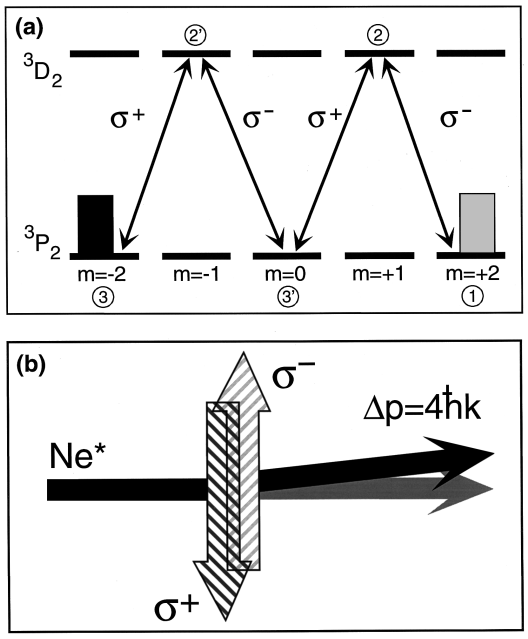

FIG. 24. The coupling scheme (a) and schematics of the setup (b) for coherent population transfer from the $m=2$ sublevel to the $m=-2$ sublevel of the $^3P_2$ level.

$$\det \mathsf{H}(t)=2\Delta_{13}\det \mathsf{H}_4(t)-\Omega_{2',3}^2\det \mathsf{H}_3(t), \qquad \text{(C4)}$$

where $\det \mathsf{H}_n$ is an n-dimensional minor of the full Hamiltonian matrix. Inspection of Eq. (C4) allows the identification of the condition for the formation of a state with zero-energy eigenvalue. The second determinant, $\det \mathsf{H}_3(t)$, relates to the three-level system ($m=-2$, $m=0$, and $m=-1$ in the $^2P_2$ and $^3D_2$ levels, respectively). It is known from the previous discussion that a state with zero-energy eigenvalue exists if the laser frequencies are in two-photon resonance with the $m=-2$ and $m=0$ states. This is in fact guaranteed, since the photons of different polarization are derived from the same laser beam, provided the laser beams cross the atomic beam at a right angle to eliminate Doppler shift. Such a shift would be different for the two beams of different polarization. We need not evaluate the first determinant, provided that four-photon resonance is also established. If $\Delta_{1,3'}=0$, we also have $\Delta_{1,5}=0$, and there exists a dressed eigenstate with zero eigenvalue, i.e., an adiabatic transfer path. Numerical modeling of the evolution of the population in the various levels, shown in Fig. 25, confirms this conclusion. The transient population of the states $m=-1$ and $m=+1$ in the $^3D_2$ level is negligibly small. It is not surprising that as much as 30% of the population resides in the level $m=0$ ($^3P_2$) at intermediate times. Since this level is metastable and there are no processes that interrupt the coherent evolution, all of this population is eventually transferred to the state $m=+2(^3P_2)$.

3. Deflection of an atomic beam by coherent momentum transfer

An experimental setup to demonstrate coherent transfer without changing the quantum state of the atom

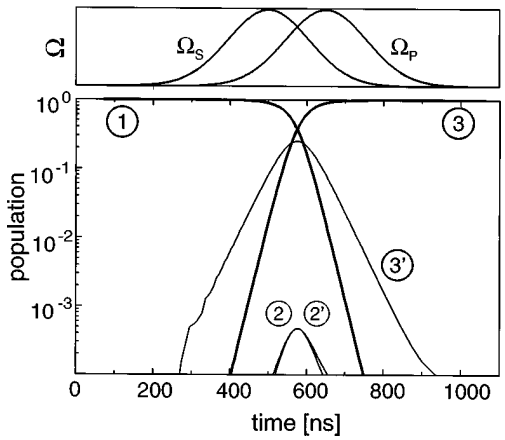

FIG. 25. Evolution of the population in the various sublevels (see Fig. 24), calculated for a laser intensity of 86 W/cm^2, corresponding to a Rabi frequency of 4×10^9 rad/s.

is shown in Fig. 26. After the transfer of the atoms from the $m=-2$ to the $m=+2$ state (involving four photons), they are transferred back to the $m=-2$ state (involving again four photons). A total momentum of $8\hbar k$ can be transferred (in the same direction) if the spatial separation of the laser beams, their polarization, and the direction of propagation are appropriately arranged. The setup of Fig. 26 involves a polarizing beam splitter, a quarter wave plate, and two cat's-eye arrangements (these combine a focusing lens in front of a mirror and act to return parallel beams of light as parallel but offset beams). The overlap of the laser beams is controlled by the (smaller) cat's eye shown in the lower right corner, while the distance between the two transfer zones is controlled by the (larger) cat's eye shown in the upper left corner.

There is no need to prepare the atoms in the $m=-2$ sublevel by a separate laser before they reach the

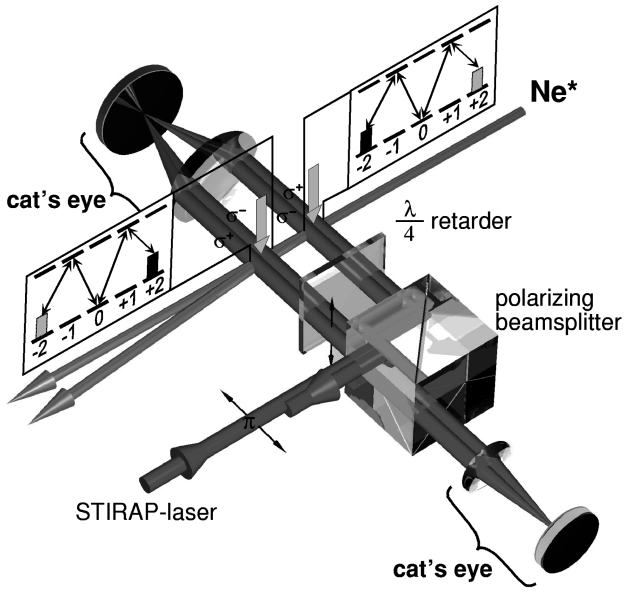

FIG. 26. View of the arrangement of optical elements used to set up a dual deflection zone, based on the coupling scheme shown in Fig. 24, derived from a single laser beam.

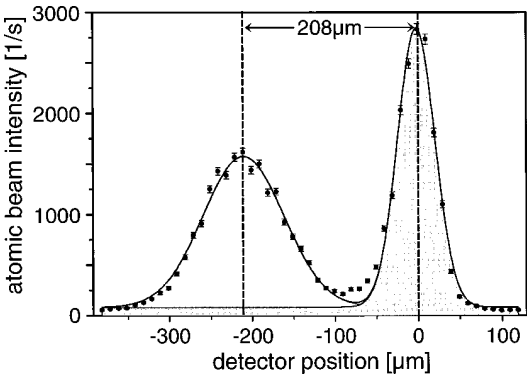

FIG. 27. Deflection of a beam of ^{20}Ne atoms by coherent momentum transfer. The narrow, undeflected beam profile is that for the undeflected ^{22}Ne isotope. The profile of the deflected beam is broader than that of the undeflected one because of the finite width of the longitudinal velocity distribution of the atoms in the beam.

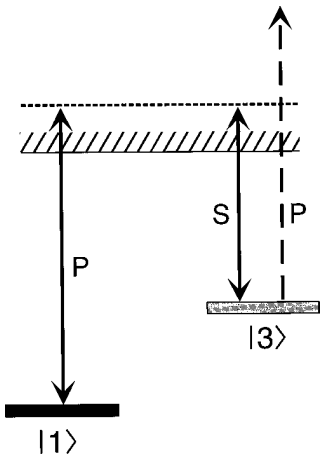

FIG. 28. The coupling scheme for population transfer via STIRAP, from an initial state $|1\rangle$, through a continuum of intermediate states, to a final state $|3\rangle$, showing final-state photoionization loss channel due to pump pulse.

transfer zones. Since the atoms are initially exposed to the σ^- radiation, the population of all levels other than $m=-2$ is depleted by optical pumping before they reach the region where the two laser beams overlap.

The profile of the atomic beam, detected by a channeltron behind a 10-μm slit 82 cm downstream from the transfer zone, is shown in Fig. 27. The ^{22}Ne atoms do not interact with the radiation field. They are detected on the atomic-beam axis. The width of the peak is determined by the geometric collimation of the atomic beam. All of the ^{20}Ne atoms are deflected. As shown in Fig. 27, the profile of the deflected beam is fully separated from the primary beam. The width of the deflected beam is broader, since the coherent momentum transfer perpendicular to the atomic beam axis is precisely $8\hbar k$, but the momentum distribution parallel to the atomic-beam axis is determined by the velocity distribution of the atoms. A time-of-flight analysis of the deflected peak would show a peak, the width of which is similar to that of the undeflected ^{22}Ne atoms, with a position that changes with the flight time (i.e., with the velocity parallel to the beam axis).

Comparison of the area of the deflected and undeflected beams allows the calibration of the efficiency of the transfer. The natural abundance of the ^{22}Ne isotope is 9.5%. Assuming uniform population of the m sublevels of the $^3P_2$ level, 20% of the atoms in that state are in the $m=+2$ state. Due to the optical pumping process, this state received an additional 4.1% of the population. Therefore the ratio of the areas of the deflected and undeflected beam should be $\gamma=2.02{:}1$ for a transfer efficiency of unity. A background count rate of about 100 s^{-1} (indicated by the thin line in Fig. 27) needs to be subtracted from the signals. It results from the emission of vuv photons from the nozzle. This radiation is diffracted by the 25-μm collimating slit. The zero-order maximum of the diffracted light has a width of 2.8 mm at the plane of the detector and contributes to a background signal that is nearly constant over the relevant area shown. After correction for this background signal, the ratio of peak areas is $\gamma=(1.54\pm0.06){:}1$, which corresponds to a reflectivity of a single transfer zone of $(76\pm3)\%$. Increasing the power density from 0.31 W/cm^2 to 6.2 W/cm^2 would yield a reflectivity exceeding 99% (see also Fig. 25). Although some energy due to photon recoil is added to the particle, this mirror can be used in an atom-optics experiment (e.g., in an atom interferometer) because coherence is preserved.

APPENDIX D: CONTINUUM TRANSFER

After successful implementation of efficient population transfer mediated by coupling of the initial and final states to a discrete intermediate state with a finite lifetime (the decay of which does not affect the transfer), it is an interesting question whether or not the coupling may also be mediated via a continuum (see Fig. 28).

For some time it has been known that coherent effects can be important for interactions that proceed through an autoionizing state (i.e., a bound state embedded in a continuum) (Knight, 1984, 1990; Dai and Lambropoulos, 1987).

The processes discussed in the previous sections involve intermediate states whose lifetimes were of the order of 10 to 100 ns, while the interaction times with the lasers spanned a similar range from 5 to 200 ns. When an electron is excited to an unstructured ionization continuum (a "flat" continuum with no narrow structure related to autoionizing levels) with an energy in excess of 1 meV, it departs from the vicinity of the core in less than 10^{-15} s. The question whether this situation is prohibitive to coherent population transfer or not has attracted considerable theoretical interest.[6]

[6]Among those who have studied this problem are Carroll and Hioe (1992), Nakajima *et al.*, (1994), van Enk, Zhang, and Lambropoulos (1995), Nakajima and Lambropoulos (1996), Yatsenko *et al.* (1997), Vitanov and Stenholm (1997), Hioe and Carroll (1997), Paspalakis, Protopapas, and Knight (1997).

In brief, Carroll and Hioe (1992) found that, for a suitably structured continuum, it would be possible to have STIRAP produce efficient population transfer via a continuum. They approximated the continuum by artificially discretizing it, but they considered the limit where the level spacing approaches zero. Although this seems a reasonable approach at first glance, such a continuum has coherence properties [e.g., recurrences in the case of wave-packet formation (Eberly, Yeh, and Bowden, 1982; Yeh, Bowden, and Eberly, 1982)], which are absent in a structureless continuum.

Subsequently it was found that the main limitation of continuum STIRAP was the Stark shift of the bound levels due to interaction with the continuum (Nakajima and Lambropoulos, 1996). Such shifts can be compensated either by a third "control" laser (Yatsenko *et al.*, 1997) or by using chirped pulses (Paspalakis *et al.*, 1997) in order to maintain the two-photon resonance, a prerequisite to the formation of a trapped state. Some detuning off the two-photon resonance may also help to offset the detrimental effect of the Stark shift (Hioe and Carroll, 1997; Yatsenko *et al.*, 1997).

Another, more obvious, limitation is the fact that the pump laser may remove the population that has been transferred to the final level by ionization (see Fig. 28). Judicious choice may reduce the detrimental effect of this incoherent loss channel, but it cannot be eliminated altogether. Experiments to test continuum STIRAP are presently under way in Kaiserslautern (Halfmann *et al.*, 1998).

REFERENCES

Alzetta, G., A. Gozzini, L. Moi, and G. Orriols, 1976, "An experimental method for the observation of r.f. transitions and laser beat resonances in oriented Na vapour," Nuovo Cimento B **36**, 5–20.

Arimondo, E., 1996, "Coherent population trapping in laser spectroscopy," Prog. Opt. **35**, 259–356.

Arimondo, E., and G. Orriols, 1976, "Non-absorbing atomic coherences by coherent two-photon transition in a three-level optical pumping," Nuovo Cimento **17**, 333–338.

Bergmann, K., and B. W. Shore, 1995, *Molecular Dynamics and Spectroscopy by Stimulated Emission Pumping* (World Scientific, Singapore).

Boller, K. J., A. Imamoglu, and S. E. Harris, 1991, "Observation of electromagnetically induced transparency," Phys. Rev. Lett. **66**, 2593–2596.

Broers, B., H. B. van Linden van den Heuvell, and L. D. Noordam, 1992, "Efficient population transfer in a three-level ladder system by frequency-swept ultrashort laser pulses," Phys. Rev. Lett. **69**, 2062–2065.

Carroll, C. E., and F. T. Hioe, 1987, "Three-state model driven by two laser beams," Phys. Rev. A **36**, 724–729.

Carroll, C. E., and F. T. Hioe, 1988, "Three-state systems driven by resonant optical pulses of different shapes," J. Opt. Soc. Am. B **5**, 1335–1340.

Carroll, C. E., and F. T. Hioe, 1989, "Two-photon resonance in three-state model driven by two laser beams," J. Phys. B **22**, 2633–2647.

Carroll, C. E., and F. T. Hioe, 1990, "Analytic solutions for three-state systems with overlapping pulses," Phys. Rev. A **42**, 1522–1531.

Carroll, C. E., and F. T. Hioe, 1992, "Coherent population transfer via the continuum," Phys. Rev. Lett. **68**, 3523–3526.

Chelkowski, S., and A. D. Bandrauk, 1997, "Raman chirped adiabatic passage: A new method for selective excitation of high vibrational states," J. Raman Spectrosc. **28**, 459–466.

Chelkowski, S., and G. N. Gibson, 1995, "Adiabatic climbing of vibrational ladders using Raman transitions with a chirped pump laser," Phys. Rev. A **52**, 3417–3420.

Dai, H. C., and R. W. Field, 1994, Eds., *Molecular Dynamics and Spectroscopy by Stimulated Emission Pumping* (World Scientific, Singapore).

Dai, B.-N., and P. Lambropoulos, 1987, "Laser-induced autoionizinglike behavior, population trapping, and stimulated Raman process in real atoms," Phys. Rev. A **36**, 5205–5208.

Dittmann, P., F. P. Pesl, J. Martin, G. W. Coulston, G. Z. He, and K. Bergmann, 1992, "The effect of vibrational excitation $(3 \leqslant v'' \leqslant 19)$ on the reaction $Na_2(v'')+Cl \rightarrow NaCl+Na^*$," J. Chem. Phys. **97**, 9472–9475.

Eberly, J. H., J. J. Yeh, and C. M. Bowden, 1982, "Interrupted coarse-grained theory of quasi-continuum photoexcitation," Chem. Phys. Lett. **86**, 76–80.

Feller, D., E. D. Glendening, E. A. McCullough, Jr., and R. J. Miller, 1993, "A comparison of unrestricted Hartree-Fock and restricted open-shell Hartree-Fock-based methods for determining the magnetic hyperfine parameters of NO $(X^2\text{-Pi})$," J. Chem. Phys. **99**, 2829–2840.

Fewell, M., B. W. Shore, and K. Bergmann, 1997, "Coherent population transfer among three states: Full algebraic solutions and the relevance of non adiabatic processes to transfer by delayed pulses," Aust. J. Phys. **50**, 281–304.

Fleischhauer, M., C. H. Keitel, M. O. Scully, C. Su, B. T. Ulrich, and S.-Y. Zhu, 1992, "Resonantly enhanced refractive index without absorption via atomic coherence," Phys. Rev. A **46**, 1468–1487.

Gaubatz, U., P. Rudecki, M. Becker, S. Schiemann, M. Kulz, and K. Bergmann, 1988, "Population switching between vibrational levels in molecular beams," Chem. Phys. Lett. **149**, 463–8.

Gaubatz, U., P. Rudecki, S. Schiemann, and K. Bergmann, 1990, "Population transfer between molecular vibrational levels. A new concept and experimental results," J. Chem. Phys. **92**, 5363–5376.

Goldner, L. S., C. Gerz, R. J. C. Spreeuw, S. L. Rolston, C. I. Westbrook, W. D. Phillips, P. Marte, and P. Zoller, 1994a, "Coherent transfer of photon momentum by adiabatic following in a dark state," Quantum Opt. **6**, 387–389.

Goldner, L. S., C. Gerz, R. J. Spreeuw, S. L. Rolston, C. I. Westbrook, W. D. Phillips, P. Marte, and P. Zoller, 1994b, "Momentum transfer in laser-cooled cesium by adiabatic passage in a light field," Phys. Rev. Lett. **72**, 997–1000.

Guerin, S., 1997, "Complete dissociation by chirped laser pulses designed by adiabatic Floquet analysis," Phys. Rev. A **56**, 1458–1462.

Halfmann, T., and K. Bergmann, 1996, "Coherent population transfer and dark resonances in SO_2," J. Chem. Phys. **104**, 7068–7072.

Halfmann, T., L. P. Yatsenko, M. Shapiro, B. W. Shore, and K. Bergmann, 1998, "Population trapping and laser-induced continuum structure in helium: Experiment and Theory," Phys. Rev. A **58**, R46–R49.

Hamilton, C. H., J. L. Kinsey, and R. W. Field, 1986, "Stimulated emission pumping: New methods in spectroscopy and molecular dynamics," Annu. Rev. Phys. Chem. **37**, 493–524.

Harris, S. E., 1993, "Electromagnetically induced transparency with matched pulses," Phys. Rev. Lett. **70**, 552–555.

Harris, S. E., 1994, "Refractive-index control with strong fields," Opt. Lett. **19**, 2018–2020.

Harris, S. E., 1997, "Electromagnetically Induced Transparency," Phys. Today **50**, No. 7, 36–42.

Harris, S. E., J. E. Field, and A. Imamoglu, 1990, "Nonlinear optical processes using electromagnetically induced transparency," Phys. Rev. Lett. **64**, 1107–1110.

Herzberg, G., 1950, *Molecular Spectra and Molecular Structure I. Spectra of Diatomic Molecules* (Van Nostrand, N.Y.).

Hioe, F. T., 1983, "Theory of generalized adiabatic following in multilevel systems," Phys. Lett. A **99**, 150.

Hioe, F. T., 1984, "Linear and nonlinear constants of motion for two-photon processes in three-level systems," Phys. Rev. A **29**, 3434–3436.

Hioe, F. T., and C. E. Carroll, 1988, "Coherent population trapping in N-level quantum systems," Phys. Rev. A **37**, 3000–3005.

Hioe, F. T., and C. E. Carroll, 1996, "Population transfer and pulse propagation in certain closed-loop systems," Phys. Lett. A **220**, 49–54.

Hioe, F. T., and C. E. Carroll, 1997, "Solitary waves and atomic population transfer via the continuum," Phys. Rev. A **56**, 2292–2298.

Hioe, F. T., and J. H. Eberly, 1984, "Multiple-laser excitation of multilevel atoms," Phys. Rev. A **29**, 1164–1167.

Kasapi, A., M. Jain, G. Y. Yin, and S. E. Harris, 1995, "Electromagnetically induced transparency: Propagation dynamics," Phys. Rev. Lett. **74**, 2447–2450.

Kasevich, M., and S. Chu, 1991, "Atomic interferometry using stimulated Raman transitions," Phys. Rev. Lett. **67**, 181–184.

Knight, P. L., 1984, "Laser-induced continuum structure," Comments At. Mol. Phys. **15**, 193–214.

Knight, P. L., M. A. Lauder, and B. J. Dalton, 1990, "Laser-induced continuum structure," Phys. Rep. **190**, 1–61.

Kuhn, A., S. Schiemann, G. Z. He, G. Coulston, W. S. Warren, and K. Bergmann, 1992, "Population transfer by stimulated Raman scattering with delayed pulses using spectrally broad light," J. Chem. Phys. **96**, 4215–4223.

Kuhn, A., S. Steuerwald, and K. Bergmann, 1998, "Coherent population transfer in NO with pulsed lasers: The consequences of hyperfine structure, Doppler broadening and electromagnetically induced absorption," Eur. Phys. J. D **1**, 59–70.

Kuklinski, J. R., U. Gaubatz, F. T. Hioe, and K. Bergmann, 1989, "Adiabatic population transfer in a three-level system driven by delayed laser pulses," Phys. Rev. A **40**, 6741–6744.

Kulin, S., B. Saubamea, E. Peik, J. Lawall, T. Hujmans, M. Leduc, and C. Cohen-Tannoudji, 1997a, "Coherent manipulation of atomic wave packets by adiabatic transfer," Phys. Rev. Lett. **78**, 4815–4188.

Kulin, S., B. Saubamea, E. Peik, J. Lawall, T. Hujmans, M. Leduc, and C. Cohen-Tannoudji, 1997b, "Coherent manipulation of atomic wave packets by adiabatic transfer," Phys. Rev. Lett. **78**, 4815–4188.

Kulz, M., A. Kortyna, M. Keil, B. Schellhaass, and K. Bergmann, 1995, "On the vibrational dependence of electron impact ionization of diatomic molecules," Z. Phys. D **33**, 109–117.

Laine, T. A., and S. Stenholm, 1996, "Adiabatic processes in three-level systems," Phys. Rev. A **53**, 2501–2512.

Lawall, J., S. Kulin, B. Saubamea, N. Bigelow, M. Leduc, and C. Cohen-Tannoudji, 1996, "Subrecoil laser cooling into a single wavepacket by velocity-selective coherent population trapping followed by adiabatic passage," Laser Phys. **6**, 153–158.

Lindinger, A., M. Verbeek, and H.-G. Rubahn, 1997, "Adiabatic population transfer by acoustooptically modulated laser beams," Z. Phys. D **39**, 93–100.

Lukin, M. D., M. O. Scully, G. R. Welch, E. S. Fry, L. Hollberg, G. G. Padmabandu, H. G. Robinson, and A. S. Zibrov, 1996, "Lasing without inversion: the road to new short-wavelength lasers," Laser Phys. **6**, 436–447.

Malinovsky, V. S., and D. J. Tannor, 1997, "A simple and robust extension of STIRAP to N-level sytems," Phys. Rev. A **56**, 4929–4937.

Marte, P., P. Zoller, and J. L. Hall, 1991, "Coherent atomic mirrors and beam splitters by adiabatic passage in multilevel systems," Phys. Rev. A **44**, R4118–4121.

Martin, J., B. W. Shore, and K. Bergmann, 1996, "Coherent population transfer in multilevel systems with magnetic sublevel. III. Experimental results," Phys. Rev. A **54**, 1556–1569.

Messiah, A., 1962, *Quantum Mechanics* (North-Holland/Elsevier Science, New York).

Miller, R. J., and D. Feller, 1994, "Comment on the hyperfine structure of the $X^2\Pi$ ground state of nitric oxide," J. Chem. Phys. **98**, 10 375.

Nakajima, T., and P. Lambropoulos, 1996, "Population transfer through an autoionizing state by pulse delay," Z. Phys. D **36**, 17–22.

Nakajima, T., M. Elk, J. Zhang, and P. Lambropoulos, 1994, "Population transfer through the continuum," Phys. Rev. A **50**, R913–R916.

Oreg, J., F. T. Hioe, and J. H. Eberly, 1984, "Adiabatic following in multilevel systems," Phys. Rev. A **29**, 690–697.

Oreg, J., K. Bergmann, B. W. Shore, and S. Rosenwaks, 1992, "Population transfer with delayed pulses in four-state systems," Phys. Rev. A **45**, 4888–4896.

Padmabandu, G. G., G. R. Welch, I. N. Shubin, E. S. Fry, D. E. Nikonov, M. D. Lukin, and M. O. Scully, 1996, "Laser oscillation without population inversion in a sodium atomic beam," Phys. Rev. Lett. **76**, 2053–2056.

Parkins, A. S., P. Marte, P. Zoller, and H. J. Kimble, 1993, "Synthesis of arbitrary quantum states via adiabatic transfer of Zeeman coherence," Phys. Rev. Lett. **71**, 3095–3102.

Paspalakis, E., M. Protopapas, and P. L. Knight, 1997, "Population transfer through the continuum with temporally delayed chirped laser pulses," Opt. Commun. **142**, 34–40.

Pillet, P., C. Valentin, R.-L. Yuan, and J. Yu, 1993, "Adiabatic population transfer in a multilevel system," Phys. Rev. A **48**, 845–848.

Romanenko, V. I., and L. P. Yatsenko, 1997, "Adiabatic population transfer in the three-level lambda-system: two-photon lineshape," Opt. Commun. **140**, 231–236.

Schiemann, S., A. Kuhn, S. Steuerwald, and K. Bergmann, 1993, "Efficient coherent population transfer in NO Molecules using pulsed lasers," Phys. Rev. Lett. **71**, 3637–3640.

Scully, M. O., 1991, "Enhancement of the index of refraction via quantum coherence," Phys. Rev. Lett. **67**, 1855–1858.

Scully, M. O., and M. Fleischhauer, 1994, "Lasers without inversion," Science **263**, 337–338.

Scully, M. O., S.-Y. Zhu, and A. Gavrielides, 1989, "Degenerate quantum-beat laser: Lasing without inversion and inversion without lasing," Phys. Rev. Lett. **62**, 2813–2816.

Shore, B. W., 1990, *The Theory of Coherent Atomic Excitation* (Wiley, New York).

Shore, B. W., 1995, "Examples of counter-intuitive physics," Contemp. Phys. **36**, 15–28.

Shore, B. W., K. Bergmann, A. Kuhn, S. Schiemann, J. Oreg, and J. H. Eberly, 1992, "Laser-induced population transfer in multistate systems: A comparative study," Phys. Rev. A **45**, 5297–5300.

Shore, B. W., K. Bergmann, J. Oreg, and S. Rosenwaks, 1991, "Multilevel adiabatic population transfer," Phys. Rev. A **44**, 7442–7447.

Smith, A. V., 1992, "Numerical studies of adiabatic population inversion in multilevel system," J. Opt. Soc. Am. B **9**, 1543–1551.

Suptitz, W., B. C. Duncan, and P. L. Gould, 1997, "Efficient 5D excitation of trapped Rb atoms using pulses of diode-laser light in the counterintuitive order," J. Opt. Soc. Am. B **14**, 1001–1008.

Theuer, H., and K. Bergmann, 1998, "Atomic beam deflection by coherent momentum transfer and the dependence on weak magnetic fields," Eur. Phys. J. D (to be published).

van Enk, S. J., J. Zhang, and P. Lambropoulos, 1995, "Coherent effects through the continuum: Transparency, population trapping and amplification without inversion through autoionizing resonances," Appl. Phys. B: Lasers Opt. **60**, S141–152.

Vitanov, N. V., and S. Stenholm, 1996, "Non-adiabatic effects in population transfer in three-level systems," Opt. Commun. **127**, 215–222.

Vitanov, N. V., and S. Stenholm, 1997, "Population transfer by delayed pulses via continuum states," Phys. Rev. A **56**, 741–747.

Walser, R., J. I. Cirac, and P. Zoller, 1996, "Magnetic Tomography of a Cavity State," Phys. Rev. Lett. **77**, 2658–2661.

Weitz, M., B. C. Young, and S. Chu, 1994, "Atom manipulation based on delayed laser pulses in three- and four-level systems: Light shifts and transfer efficiencies," Phys. Rev. A **50**, 2438–2444.

Yatsenko, L. P., R. G. Unanyan, K. Bergmann, T. Halfmann, and B. W. Shore, 1997, "Population transfer through the continuum using laser-controlled Stark shifts," Opt. Commun. **135**, 406–412.

Yeh, J. J., C. M. Bowden, and J. H. Eberly, 1982, "Interrupted coarse grained theory of unimolecular relaxation and stimulated recurrences in photoexcitation of a quasicontinuum," J. Chem. Phys. **76**, 5936–5946.